

Digital Microfluidics Chips for Execution and Real-Time Monitoring of Multiple
Ribozymatic Cleavage Reactions

Alen Nellikulam Davis

A Thesis
in
The Department
of
Electrical and Computer Engineering

Presented in Partial Fulfillment of the Requirements
for the Degree of Master of Applied Science at
Concordia University
Montreal, Quebec, Canada

November 2020

© Alen Nellikulam Davis, 2020

CONCORDIA UNIVERSITY
SCHOOL OF GRADUATE STUDIES

This is to certify that the thesis prepared

By: Alen Nellikulam Davis

Entitled: Digital Microfluidics Chips for Execution and Real-Time Monitoring of Multiple Ribozymatic Cleavage Reactions

and submitted in partial fulfillment of the requirements for the degree of

Master of Applied Science (Electrical and Computer Engineering)

complies with the regulations of this University and meets the accepted standards with respect to originality and quality.

Signed by the final examining committee:

_____	Chair
Dr. M. Kahrizi	
_____	External Examiner
Dr. P. Joyce (CHEM)	
_____	Internal Examiner
Dr. M. Kahrizi	
_____	Co-Supervisor
Dr. N. Kharma	
_____	Co-Supervisor
Dr. S. Shih	

Approved by: _____
Dr. Y.R. Shayan, Chair
Department of Electrical and Computer Engineering

November 23rd, 2020

Dr. Mourad Debbabi, Interim Dean,
Gina Cody School of Engineering and
Computer Science

ABSTRACT

Digital Microfluidics Chips for Execution and Real-Time Monitoring of Multiple Ribozymatic Cleavage Reactions

Alen Nellikulam Davis

Microfluidics is a technology that facilitates the automation and miniaturization of biochemical experiments on platforms of small footprints. Among the different types of microfluidics platforms, digital microfluidics (DMF) devices execute an experiment by manipulating droplets of small volume (usually between 10^{-6} and 10^{-9} L) on an array of electrodes using the principles of electrowetting. These DMF chips provide control over individual droplets which enables users to perform multi-step or entirely different experiments without the need for any chip reconfiguration. DMF platforms can also be reused multiple times and can be integrated with other devices like a plate reader to monitor the progress of reactions in real-time. These advantages of DMF devices make them an ideal choice to automate end-end biochemical experiments.

In this work, we describe the design and performance of two digital microfluidics (DMF) chips capable of executing multiple ribozymatic reactions, with proper controls, in response to short single-stranded DNA inducers. Since the fluorescence output of a reaction is measurable directly from the chip, without the need for gel electrophoresis, a complete experiment, involving up to eight reactions (per chip) can be carried out reliably, relatively quickly and efficiently. The ribozymes can also be used as biosensors of the concentration of oligonucleotide inputs, with high

sensitivity, low limits of quantification and of detection, and excellent signal-to-noise ratio. The presented chips are readily usable devices that can be used to automate, speed-up and reduce the costs of ribozymatic reaction experiments.

Acknowledgements

I would like to express my very great appreciation to Dr. Nawwaf Kharma and Dr. Steve Shih, my research supervisors, for their patience, encouragement, and useful guidance for this research work. I would like to thank Dr. Jonathan Perreault (INRS) for his support, assistance, and guidance throughout my research, which helped me to complete all the works successfully. My thanks are also extended to Mr. Jay Kapadia and Mr. Emre Yurdusev for their help in all the bench experiments and to Ms. Kenza Semlali, who helped me with the microfluidics related assays. Finally, I wish to thank my parents for their support and encouragement throughout my life and university studies.

Overview of Chapters

This thesis describes the project that I conducted for the completion of my Master's in Applied Science in electrical and computer engineering under the supervision of Dr. Nawwaf Kharm and Dr. Steve Shih at Concordia University. In this project, we aimed to design and develop a digital microfluidics chip to conduct and monitor ribozyme cleavage experiments in an automated fashion. The thesis introduces the structure and activity of ribozymes and also gives an overview of microfluidics. After reviewing different ways of reporting the cleavage of the ribozyme, in this thesis, we describe a straightforward experiment to monitor the progress of these cleavage reactions. Finally, the thesis elaborates the protocols followed in carrying out different stages within the project and showcase the obtained results.

Chapter 1 introduces ribozymes, their structure and activity to the readers. The chapter also provides an insight into microfluidic technology and different types of microfluidic platforms. Additionally, in this chapter, we review different experiments to monitor ribozyme cleavage experiments on microfluidic devices.

Chapter 2 describes the methodology and protocols followed in the project in order to perform the reactions both on a lab bench and on digital microfluidics chip.

Chapter 3 demonstrates the results generated from all the experiments conducted as part of the project. The chapter also describes the data analysis and inferences made from the obtained results.

Chapter 4 summarizes the results and reiterates the advantages of performing these ribozyme cleavage experiments on the digital microfluidics platforms.

Chapter 5 discusses the improvements that can be incorporated into the project for future work.

Contents

List of Figures	ix
List of Tables	x
Abbreviations	xi
Chapter 1: Introduction	1
1.1 Nucleic acids	1
1.1.1 Deoxyribonucleic acid	1
1.1.2 Ribonucleic acid.....	3
1.2 Ribozymes	3
1.3 Hammerhead ribozymes	4
1.4 Review of conventional methods of monitoring ribozyme cleavage kinetics	5
1.4.1 Radioactivity	6
1.4.2 Fluorescence.....	6
1.4.3 Toehold mediated strand displacement reaction.....	8
1.4.4 Automation of ribozyme kinetic measurements	8
1.5 Microfluidics	9
1.5.1 Channel-based microfluidics devices	9
1.5.2 Droplet-in-Channel microfluidics devices.....	10
1.5.3 Digital microfluidics devices.....	13
1.6 Review of enzymatic and ribozymatic experiments on microfluidic devices	15
1.6.1 Enzymatic Assays on Microfluidic Devices	15
1.6.2 Ribozyme on Microfluidic Platforms	17
1.7 Purpose of the Research	17
Chapter 2: Experimentation and Methodology	19
2.1 Benchtop experiments	19
2.1.1 Ribozyme assembly and transcription	19
2.1.2 Preparation of probe	20
2.1.3 Benchtop ribozyme cleavage assay	22
2.2 DMF chip experiments	22
2.2.1 DMF chip fabrication.....	22
2.2.2 Automation system for the DMF chip	24
2.2.3 DMF chip ribozyme cleavage assay	24

Chapter 3: Results and Discussion	26
3.1 DMF chip design and architecture	26
3.2 Benchtop and DMF chip monitoring of ribozyme cleavage kinetics	30
3.3 Benchtop and DMF chip analysis of ribozyme as a biosensor	36
4.4 Multiple ribozyme cleavage assays on a DMF chip	40
Chapter 4: Summary and Conclusion	44
Chapter 5: Future Work	46
References	47
Appendices	60
Appendix 1: User Manual	60

List of Figures

Figure 1: Nucleic acid structure.....	2
Figure 2: Consensus of hammerhead ribozyme.....	5
Figure 3: Fluid flow manipulation in channel microfluidics.....	10
Figure 4: Droplet formation in droplet-in-channel microfluidics.....	11
Figure 5: Droplet diffusion in droplet-in-channel devices.....	12
Figure 6: Mixing reagent droplets in droplet-in-channel microfluidics.....	12
Figure 7: Side view and top view of DMF chip with a droplet.....	14
Figure 8: Schematic representation of primerize assembly design.....	19
Figure 9: Preparation of the quenched probe.....	21
Figure 10: A schematic of the DMF chip and device operations.....	23
Figure 11: Overview of the ribozyme cleavage assay on a digital microfluidic (DMF) chip.....	27
Figure 12: On-chip fluorescence intensity measurements.....	30
Figure 13: Comparison of the ribozyme well-plate and DMF chip assay.....	32
Figure 14: Analysis of change in fluorescence in the ribozyme cleavage experiment.....	33
Figure 15: Well-Plate and DMF chip kinetics of the ribozyme cleavage assay.....	35
Figure 16: Monitoring the progress of ribozyme cleavage reactions with varying input concentrations.....	37
Figure 17: Analysis of ribozyme as a biosensor by activating the ribozyme with varying input concentrations.....	38
Figure 18: A schematic of a new DMF chip design to carry out eight simultaneous experiments.....	41
Figure 19: Ribozymatic assay in triplicates on a DMF chip.....	42
Figure 20: Multiple experiments performed simultaneously on a DMF chip.....	42

List of Tables

Table 1: Primers are generated by the tool Primerize for the assembly of the ribozyme.	20
Table 2: Parameters of linear regression fit to the benchtop and DMF chip negative controls...	33
Table 3: Parameters of linear regression fit to the benchtop and DMF chip positive controls.....	34
Table 4: Parameters of linear regression fit to the benchtop and DMF chip assay.	34
Table 5: Parameters of one phase decay regression fit to the benchtop and DMF chip ribozyme cleavage assay.....	35
Table 6: Parameters of sigmoidal curve fit to the ribozyme cleavage assay on benchtop and DMF chip experiments with different input concentrations.....	38

Abbreviations

AS: Assay

DMF: Digital microfluidics

DNA: Deoxyribonucleic acid

FRET: Florescence resonance energy transfer

HHR: Hammerhead ribozyme

LoD: Limit of detection

LoQ: Limit of quantification

NC: Negative control

PC: Black hole quencher

PCR: polymerase chain reaction

RNA: Ribonucleic acid

TMSDR: Toehold mediated strand displacement reaction

Chapter 1: Introduction

1.1 Nucleic acids

Nucleic acids are essential information-carrying macromolecules found in living organisms and viruses. These molecules determine the inherited characteristics of all living organisms by directing the process of protein synthesis [1]. They are composed of a series of chain-like molecules called the nucleotides. Nucleic acids can be classified into two categories, deoxyribonucleic acid (DNA) and ribonucleic acid (RNA).

1.1.1 Deoxyribonucleic acid

Deoxyribonucleic acid (DNA), the hereditary material in all living organisms is a double-helical structure composed of two anti-parallel strands, each formed by linking nucleotides. These nucleotides have three main parts; a phosphate group, a deoxyribose sugar and a nitrogenous base, which is either: A, G, C or T (adenine, guanine, cytosine, thymine) [2]. Adenine and guanine are purine bases while cytosine and thymine are pyrimidine bases. A single-stranded DNA molecule (ssDNA) is formed from a sequence of bases joined through a backbone of phosphate and deoxyribose sugar [3], [4]. Purine bases (A and G) can form hydrogen bonds with pyrimidine bases (C and T). Guanine can form three hydrogen bonds with cytosine, and adenine can form two hydrogen bonds with thymine. This complementary base pairing binds one ssDNA to another anti-parallel ssDNA strand resulting in the formation of a double-helical structure [3] (Figure 1). The

interaction also provides a mechanism for the replication of DNA and the transmission of genetic information [5].

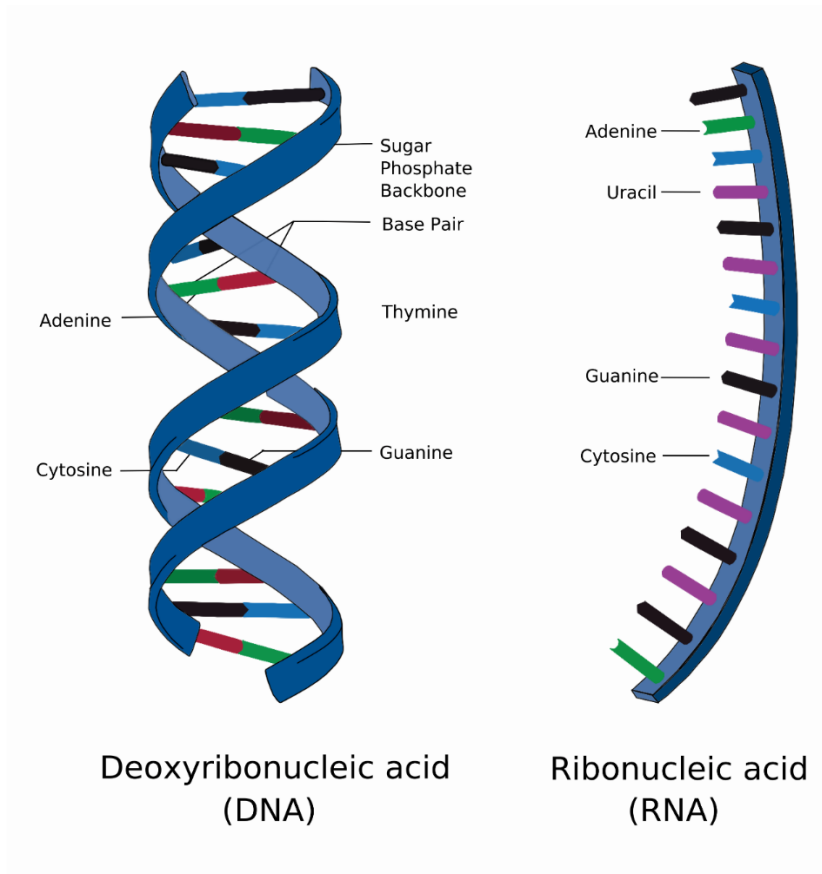


Figure 1: Nucleic acid structure.

An illustration of double helical structure of a DNA molecule (left) and a single stranded RNA molecule (right). Image adapted from [1].

1.1.2 Ribonucleic acid

Ribonucleic acid (RNA) is a single-stranded molecule formed by linking sequences of nucleotides with a backbone composed of an alternating ribose sugar and a phosphate group. RNA has all the bases of DNA except that thymine (T) residues are replaced by uracil (U) (Figure 1). Cells have different types of RNAs which include messenger RNA (mRNA), ribosomal RNA (rRNA), and transfer RNA (tRNA) [6]. The single-stranded structure of RNA makes it more flexible compared to the double-helical DNA, enabling it to form different secondary and tertiary structures [4] (Figure 1). It has also been observed that two or more such RNA structures can join together and form complex tertiary structures with different functionalities such as ligation and cleavage, which in turn can assist in catalytic reactions [7]. Such RNA molecules with catalytic properties are called ribozymes, and they play vital roles in various cellular reactions.

1.2 Ribozymes

Ribozymes are RNA molecules that can catalyze many biochemical reactions within a cell. Ribozymes were discovered in the early 1980s and demonstrated the fact that RNA molecules could act both as genetic material and biological catalysts [8], [9]. The discovery of ribozymes also provided explanations of many biological processes such as RNA splicing, transfer RNA biosynthesis and viral replication [10]. Many natural ribozymes are known to catalyze the ligation or cleavage of RNA strands after the formation of specific base pairing with the substrate along with other tertiary interactions [11], [12]. This activity of ribozymes has made it possible to use them for applications such as inactivation of specific gene transcripts leading to gene silencing [9], [13].

The secondary structure of natural ribozymes defines a catalytic core composed of conserved nucleotides, which initiate the catalysis of intramolecular reactions (except in the case

of RNase P) [9]. Ribozymes are classified as *trans*-acting and *cis*-acting, based on their activity. A *trans*-acting ribozyme binds to a distinct substrate and cuts that substrate after the formation of a catalytic core. On the other hand, the *cis*-acting ribozyme folds into a secondary structure with an active catalytic core and cuts itself. The *trans*-acting ribozymes can have multiple reactions, whereas *cis*-acting ribozymes are single turn-over enzymes [14]. Ribozymes are assigned to one of three categories: (A) self-splicing molecules, which are further classified into group I and group II introns, (B) RNase P and (C) Small catalytic RNAs of sizes ranging between 50-150 nucleotides. Among the different types of ribozymes, in this study, we focused on the activity of a *cis*-acting hammerhead ribozyme, due to its simple structure and ease of manipulation in laboratories [15].

1.3 Hammerhead ribozymes

Hammerhead ribozymes (HHR) are small catalytic RNAs ranging from 50-150 nucleotides. They were first identified by a conserved sequence motif responsible for self-cleavage in satellite RNAs of certain viruses and plant viroids [16]–[18]. A HHR catalyzes a biochemical reaction called transesterification, leading to the self-scission of the phosphodiester backbone [19], [20]. Studies suggest that this cleavage reaction requires divalent metal ions, like Mg^{2+} , which stabilize the structure of HHR molecules and thereby assist in the strand scission reaction [21], [22]. An active HHR is composed of three duplex stems that meet a conserved core of non-helical segments, and the positions of the stems and core are essential for the activity of the HHR [15], [19], [23] (Figure 2). The small size and robustness of activity of HHRs have made them into preferred ribozymes for many applications [15].

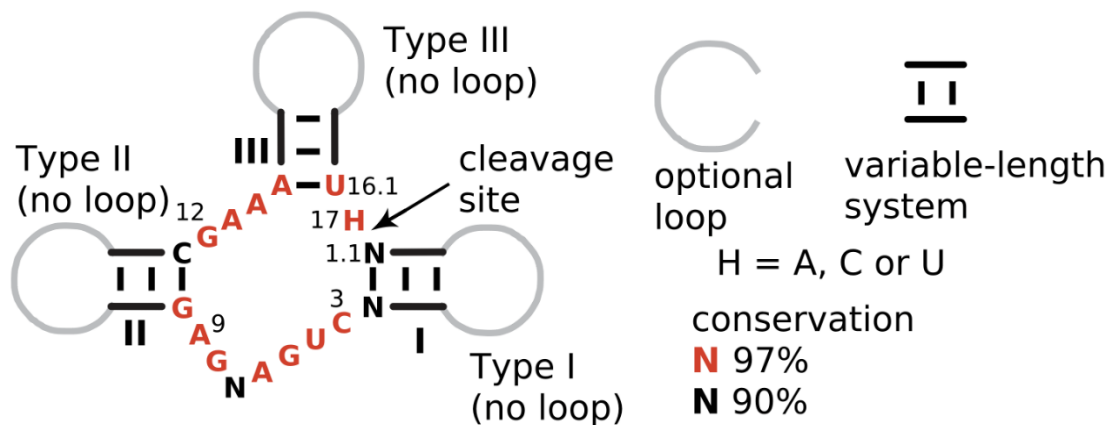


Figure 2: Consensus of hammerhead ribozyme

N represents any nucleotides. The most conserved nucleotides for the core are indicated in red, whereas nucleotides in black has a conservation of 90%. The numbers I, II, and III (in bold) represent the stem enumeration. The optional loop determines the type of hammerhead ribozyme (Type I, II or III). Figure taken from [15].

After studying the structure of natural HHRs, many synthetic HHRs have been designed to self-cleave, culminating in the release of a desired RNA strand or to act as a *trans*-acting ribozyme to cut a target RNA molecule [24]–[27]. These synthetic HHRs have also been designed to develop logical circuits, such as digital gates, which can produce outputs depending on inputs [24], [25]. In this study, we utilize a HHR that acts as a YES logic gate. When HHR is bound to an oligonucleotide (input strand), it refolds into an active state and performs a strand scission reaction, in a *cis* manner, to release a small RNA fragment (output strand).

1.4 Review of conventional methods of monitoring ribozyme cleavage kinetics

Researchers have used ribozymes for a wide variety of applications ranging from biosensing, to designing logical circuits [24]–[26], [28]. These studies required researchers to analyze and evaluate the structure and activity of a ribozyme’s cleavage for its characterization. Several

methods have been developed to carry out such studies *in vitro* and used different reporting techniques like radioactivity and fluorescence [15], [29], [30].

1.4.1 Radioactivity

The utilization of radioactivity for the *in vitro* analysis of RNA molecules is one of the most established methods [30], [31]. Here, a radioisotope of phosphorous (P32) is incorporated into the RNA molecule during transcription or post transcriptionally using a kinase enzyme [15], [31], [32]. Both procedures require the separation and purification of RNA products on polyacrylamide gels and then subsequent phosphorescence imaging-based autoradiography [15], [31], [32]. The process also involves sampling for each data point, which makes it even more cumbersome. Several other disadvantages of the radiolabeling include the short half-life of P32, additional training to handle hazardous materials, besides the radioactivity itself. Moreover, these limitations have hindered the automation of such experiments. These led researchers to develop other reporting techniques such as fluorescence for *in vitro* analysis of RNA molecules [29], [33]–[35].

1.4.2 Fluorescence

Many prominent methods utilize fluorescence resonance energy transfer (FRET) to analyze the structure and activity of ribozymes [29], [33], [34]. In these studies, researchers investigated the dynamics of *trans* cleaving hammerhead ribozymes (HHR) by attaching fluorophore-quencher pairs to the ends of the ribozyme or substrate. The cleavage of the ribozyme separates the quencher from the fluorophore resulting in a change of fluorescence, indicating the progress of the reaction [29], [33], [34]. Similar to FRET-based experiments, the kinetics of hairpin ribozyme cleavage have also been monitored using fluorescein based substrates [35]. Here, the 3' end of the substrate is labelled with fluorescein, which is quenched upon binding with the ribozyme. The quenching is induced when the guanosine at the 5' of the ribozyme is closer to the fluorescein. These techniques

are often considered an excellent alternative to the complex methods involving radioactivity. However, these methods modify the RNA molecules by the addition of fluorophore and quencher molecules. Prior studies suggest that adding these molecules can interfere with the thermodynamic stability of the nucleic acid, which in turn can impact the secondary structure and functionality of the RNA [36].

A different approach, described in [37] labels RNA molecules during *in vitro* transcription with cyanine AMP at the 5' end by utilizing a T7 ϕ 2.5 promoter. The process synthesized two novel fluorescent cyanine-AMP conjugates to prepare 5' labelled RNA for its structural and functional investigation, eliminating the need for (P32) labelling [37]. Additionally, the cyanine dyes possess excellent molecular extinction coefficients and resistance to photobleaching [38]. However, this method requires the RNA molecule to have an "AG" at its 5' end [37]. Also, in the experiment, the analysis of RNA products is performed on a gel, which becomes cumbersome for a large number of RNA samples.

Another group devised fluorescent aptamer-ribozyme architectures that facilitate the real-time measurement of the ribozyme *cis*-cleaving activity *in vitro* [11]. Here, nucleic acid molecules were engineered to be implemented as a split spinach aptamer sequence. Upon the cleavage of the ribozyme, the split aptamer sequence is made accessible to a strand displacement reaction, thereby completing the formation of the fluorescent spinach aptamer. Hence, the change in fluorescence intensity indicates the progress of the cleavage reaction [11]. However, this experiment also modifies the RNA sequence by incorporating part of the spinach aptamer into the hammerhead ribozyme, which may alter its secondary structure in a functionally relevant way.

1.4.3 Toehold mediated strand displacement reaction

In contrast to the previously mentioned reporting techniques, we used a toehold mediated strand displacement reaction (TMSDR) to report and monitor the cleavage of the ribozyme, as demonstrated in previous studies [39]. Unlike other techniques, this method links fluorophore and quencher to two different ssDNA molecules, comprising a probe, and hence has no impact on the secondary structure of the ribozyme [39]. Here, the ssDNA strand with the quencher at its 5' end is pre-annealed to the strand with the fluorophore, making up a quenched probe. When the ribozyme is cleaved, the cleaved-off strand displaces the quencher strand and binds to the probe allowing it to fluoresce. Therefore, reading fluorescence intensities is a measure of the amount of cleaved strand that is bound to the probe, which in turn, is an estimation of ribozyme cleavage.

1.4.4 Automation of ribozyme kinetic measurements

In an attempt to automate the process of monitoring the progress of a ribozyme cleavage reaction, Tracy et al. [40] carried out an experiment that demonstrated the application of chip electrophoresis with capillary sample introduction. The experiment studied the activity of a *cis*-acting ribozyme (leadzyme) that cleaves itself in the presence of Pb^{2+} ions. The ribozyme was also end-labelled (5') with fluorescein (FAM), and the progress of the reaction was monitored using laser-induced fluorescence detection. After mixing the reagents in a vial, samples were introduced automatically into the channels of a microfabricated chip. On these channels, the samples were continuously monitored using the laser-induced fluorescence technique, and a charge-coupled device (CCD) camera collected the signal. The study showed that the kinetics of a ribozyme cleavage reaction could be monitored automatically at a high sampling rate, without the need for additional sample-handling steps [40]. However, the experiment required direct labelling of RNA molecules with a fluorophore, which could impact the structure and functionality of the ribozyme. Moreover, the

experiments were carried out in a vial, and the study only automated the sampling procedure. In contrast, other automation techniques like microfluidics have provided platforms for end-end automation of biochemical experiments [41].

1.5 Microfluidics

Microfluidics is the study of the behavior and manipulation of fluids through geometrically small channels or platforms [42], [43]. It also refers to the designing and fabrication of microdevices to facilitate the automation of various lab experiments at smaller volumes. The miniaturization of these experiments on such microfabricated devices can reduce reagent consumption and allow well-controlled mixing and particle manipulation [42], [44]. Microfluidic systems can be categorized based on the flow of fluids on these devices. These include channel-based devices, droplet-in-channel microfluidics, and digital microfluidics (DMF) chips.

1.5.1 Channel-based microfluidics devices

Channel-based microfluidic systems manipulate fluids as streams in enclosed channels fabricated on a chip [43], [45], [46]. The fluid flow in these channels is generated by pressuring the pneumatic valves created by the thin membrane between the channels (Figure 3) [47]. The valves can be opened or closed by pumping air or gas using mechanical pumps, which forces the fluids in the channels to move. Attempts have also been made to achieve this motion with magnetic or electric valves [48]–[50]. However, pneumatic valves are used more widely because of their small size, low cost and robustness [51], [52]. Though these systems use diffusion [45], [46], [53] or complex structure like three valves in a row to operate in a peristaltic sequence to mix the reagents [54], these devices are the most established microfluidic platforms.

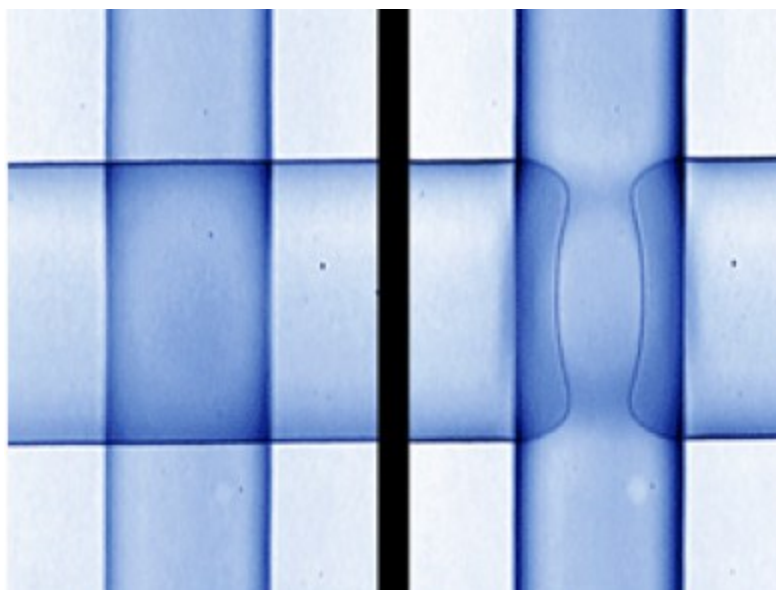


Figure 3: Fluid flow manipulation in channel microfluidics.

An illustration of a channel in its normal state (left) and deflection on the channel when the channel membrane is pressurized by pumping air or gas (right). Image taken from [47].

1.5.2 Droplet-in-Channel microfluidics devices

In droplet-in-channel microfluidics, the reagent fluids are handled as small discrete droplets in an immiscible phase, usually air or oil [55], [56]. The uniform production of droplets is an essential aspect of these systems and usually generated in the form of emulsion from two immiscible fluids such as water and oil or using air-liquid droplet systems. Different droplet formation techniques include T-junction and flow focusing [57] (Figure 4). The droplets are fused by following a passive or active mechanism. In passive fusion, the geometry of the channel is modulated to slow the downstream droplet until the upstream droplet meets it, leading to the fusion of the droplets [58] (Figure 5). At the same time, active fusion is achieved by integrating the channel with an electric field or using electric-controlled methods [59]. Some of these droplet-based devices use winding channels to mix the reagent droplets by chaotic advection (Figure 6) [60]. When compared to channel-based systems, droplet-in-channel microfluidic devices offer greater feasibility of

handling fluids at miniature volumes, provides better mixing, encapsulation, sorting and are also suitable for high throughput experiments [55], [61].

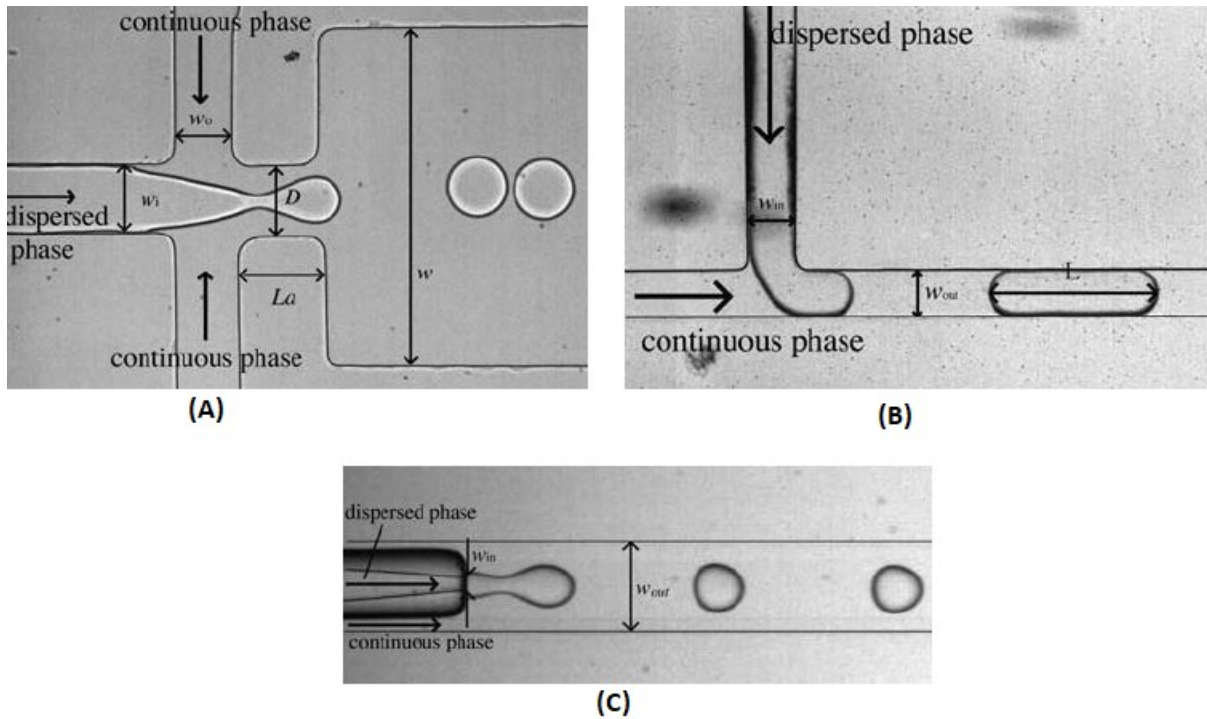


Figure 4: Droplet formation in droplet-in-channel microfluidics.

(A) Droplet production using a flow-focusing device. The two counter-streaming continuous phase flows squeeze the dispersed phase, forcing it to detach as droplets. (B) Droplet production in a T-junction, where the dispersed phase meets the continuous phase at a 90-degree T-shaped junction. (C) An example of droplet production using a co-axial injection device, where a thin round capillary produces the inner flow, thereby entering a square capillary. All images are taken from [57].

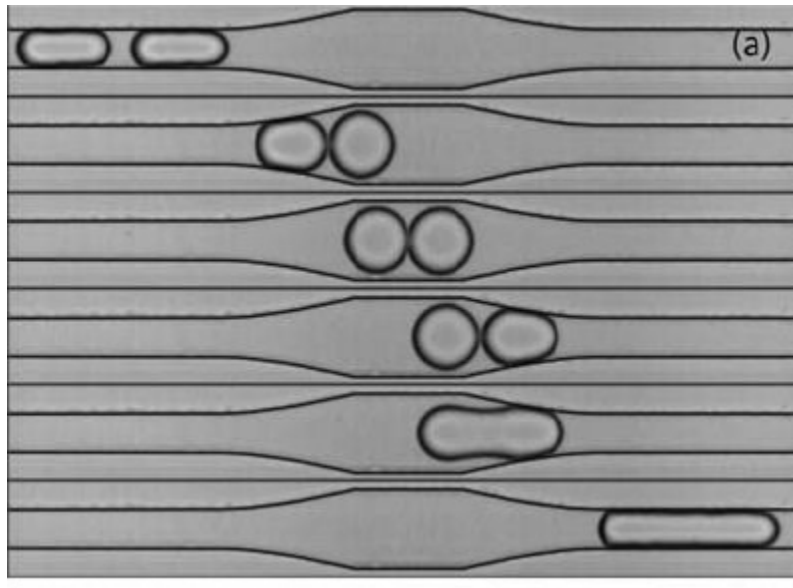


Figure 5: Droplet diffusion in droplet-in-channel devices.

The figure is a depiction of merging droplets using decompression created by the change in geometry of the channels. Here, the change in the channel's shape delays the downstream flow droplet and enables the upstream droplet to meet and merge with the downstream droplet. The image is adapted from [58].

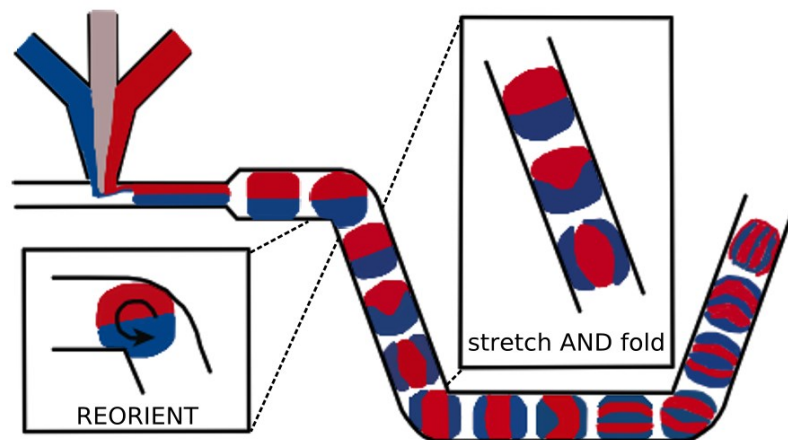


Figure 6: Mixing reagent droplets in droplet-in-channel microfluidics.

A schematic demonstration of mixing droplets in droplet-in-channel microfluidics devices by moving through winding channels. Image is taken from [60].

1.5.3 Digital microfluidics devices

Digital microfluidics is an emerging liquid handling method that manipulates liquid in discrete droplets on a microfluidic platform (with an array of electrodes) by following the principles of electrowetting [62]–[64]. These devices are composed of an open array of electrodes coated with a hydrophobic insulator. On applying a series of electric potentials on these electrodes, the droplets can be individually addressed to move, merge, split and dispense from a reservoir [65]. DMF devices primarily operate in two different configurations; a single-plate (or open) devices [66] and two-plate (or closed) devices [67]–[69]. In the two-plate configuration, the droplet is sandwiched between a top-plate and a bottom-plate. Here, the top-plate forms a ground electrode formed by a transparent and conductive layer of indium tin oxide (ITO). The bottom plate contains the array of electrodes that are actuated on the application of an electric potential. Whereas, in a one-plate device, the droplets reside on a substrate which has both actuation and ground electrodes. In both configurations, the bottom-plate electrodes are insulated with a dielectric layer and then covered with a hydrophobic coating. Although both these setups operate in the same manner, the one-plate chips are incapable of splitting and dispensing droplets. However, these open DMF platforms are well-suited for preparative applications, where the analytes are recovered after droplet actuation (Figure 7) [65]. As in the droplet-in-channel microfluidics, DMF devices automate the experiments and facilitate the reduction of reagent volume and costs. Moreover, these DMF platforms also provide control over individual droplets, which enable users to carry out complex and multi-step reactions with multiple reconfigurations [65].

In this study, we perform a ribozyme cleavage reaction on closed DMF chips because of their flexibility, portability, and easy integration with other devices such as plate readers [70]–[72]. Additionally, the top-plate provides additional protection from contamination and can thus assist in generating more reliable results.

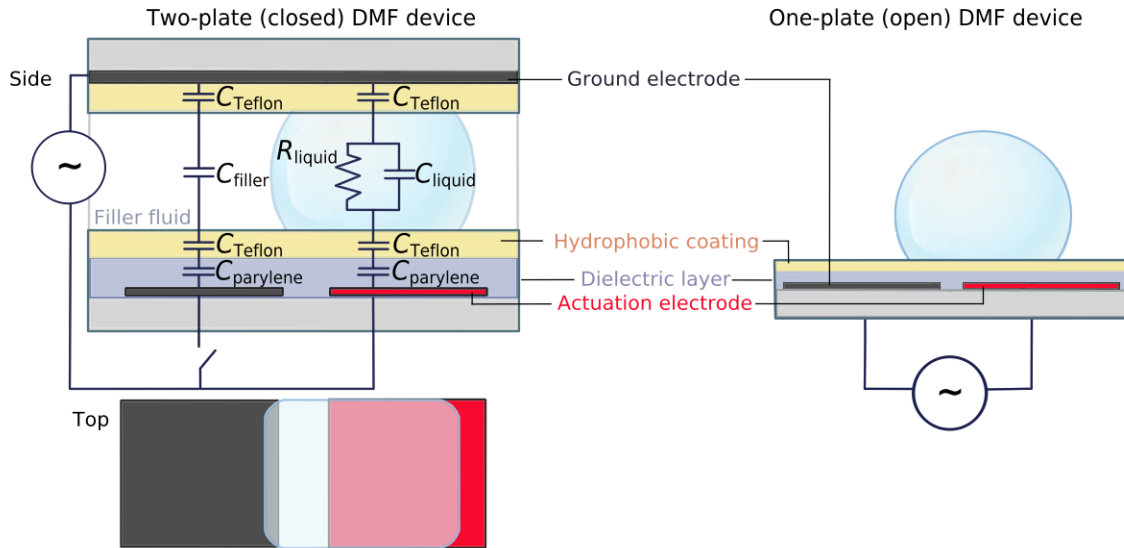


Figure 7: Side view and top view of DMF chip with a droplet.

A depiction of both the two-plate and one-plate DMF device setup with both top-view (bottom figure) and side-siew schematic. The side view of the two-plate DMF device also includes an overlaid circuit model. Image adapted from [65].

1.6 Review of enzymatic and ribozymatic experiments on microfluidic devices

Microfluidic technology has facilitated the automation of many biochemical experiments on micro-structured platforms [45], [73], [74]. Experiments on these platforms have numerous advantages including reduction in reagent usage, mitigation of losses due to sampling, development of ultra-high throughput devices, portability and faster reaction rates [20], [75], [76]. Among the different types of biochemical reactions, some researchers have also deployed experiments involving enzymes and ribozymes [45], [46], [70], [75].

1.6.1 Enzymatic Assays on Microfluidic Devices

Some of the first enzymatic assays on microfluidic platforms were performed by Hadd et al. [45], [46]. In the first experiment, a reaction between the enzyme β -galactosidase (β -Gal) and resorufin β -galactopyranoside (RBG) was performed, which resulted in the formation of a fluorescent product, resorufin [45]. The second experiment involved the analysis and electrophoretic separation of acetylcholinesterase (AChE) inhibitors on a microfabricated device. In the experiment, a reaction between thiocholine and coumarinyl phenyl maleimide, producing thioether was performed on a microfluidic chip to measure the AChE-catalyzed hydrolysis of acetylthiocholine [46]. Both the enzyme assays were performed by transporting the reagents through enclosed microchannels in a continuous flow format and using diffusion for the mixing of reagents. The experiments also utilized laser-induced fluorescence detection to monitor enzyme kinetics. A clear advantage was that these experiments exhibited a four-orders of magnitude reduction in the consumption of enzymes and substrate [45], [46]. However, the experiments had longer reaction times and often relied on a complex apparatus for fluorescence detection.

In a different experiment by Burke et al. [53], a channel-based microfabricated device with a micromixer was used to conduct a stopped-flow enzyme assay of β -galactosidase (β -Gal). The experiments proceeded by transporting the reagents through the micro-channels, which were then merged and passed through the micromixer. As in previous experiments, the progress of the enzymatic reaction was monitored using a laser-induced fluorescence detection technique. The new setup reduced the reaction time of the experiment to 60 seconds and also facilitated a reduction in reagent consumption [53]. However, these channel-based microfluidic platforms often had expensive and time-consuming fabrication procedures. Moreover, redesigning the devices to suit a different application requires a significant amount of effort and expense.

Another paradigm of the microfluidic platform, digital microfluidics (DMF), was used to carry out homogeneous enzyme assays [70]. In this approach, reagents are addressed as droplets and manipulated on a chip composed of arrays of electrodes by following the principles of electrowetting. The experiment used alkaline phosphatase as a model enzyme and converted fluorescein diphosphate to fluorescein. On the DMF chip, droplets of alkaline phosphatase were merged and mixed with droplets containing fluorescein diphosphate after which fluorescence was measured using a plate reader. The experiment demonstrated the application of digital microfluidics to the performance of enzymatic assays and the study of their kinetics. The technique also indicated that the DMF enzyme assay has a greater sensitivity than other macroscale methods, without sacrificing dynamic range [70]. A significant disadvantage of the technique is that the fabrication of such devices is a complicated and time-consuming process. However, a few rapid prototyping protocols to fabricate DMF chips have been developed by researchers [77], [78].

1.6.2 Ribozyme on Microfluidic Platforms

A recent experiment exploited a droplet-in-channel microfluidics system to isolate and select efficient ribozymes from a gene library and studied the catalytic activity of efficient *trans*-acting ribozymes under multiple-turnover conditions [79]. The experiment focused on the selection of effective *trans*-cleaving x-motif ribozymes and the operations carried out in droplets on a microfluidic device. After the selection process, additional experiments were performed for the enzymatic characterization of selected ribozymes. To achieve this, the ribozymes were mixed with a solution of fluorogenic RNA substrate labelled with a fluorophore (Atto 488) and quencher (BHQ 1) at its 5' and 3' ends, respectively. Upon binding with the ribozyme, the RNA substrate cleaves and releases either the fluorophore or the quencher strand, which in turn increases the fluorescence. The progress of the reaction is observed using a laser-induced fluorescence technique. The results from this study demonstrated the potential of microfluidic platforms to perform high throughput experiments [79]. However, this study used a complex optical setup for monitoring the kinetics of the ribozyme. Moreover, the system also lack independent control over droplets which can limit the device from performing a ribozymatic experiment with multiple steps [26] on the device.

1.7 Purpose of the Research

All the previously mentioned techniques are most often carried out on the bench and require large volumes of reagents, various consumables (plates, pipettes, and tips) and a fair bit of labor. Some experiments are performed in multiple steps and require additional pipetting. This makes the reactions prone to contamination and pipetting errors. Moreover, these techniques lack tools for automated testing and real-time monitoring of ribozyme cleavage assays.

Therefore, we propose the realization of ribozyme cleavage assays on digital microfluidics (DMF) chips, which miniaturize these experiments and facilitate their automation. On DMF chips, an experiment can be carried out in microdroplets and using small quantities of reagents. These reactions on DMF devices can potentially have faster reaction rates and increased sensitivity as shown in previous studies [70], [80]. Additionally, DMF platforms are highly flexible and portable and can readily be integrated with machines like plate readers to automate entire experiments.

The objectives of this thesis are:

- Objective 1: To design a DMF chip (or more) that can be utilized to conduct a cleavage assay of an RNA/DNA-inducible *cis*-acting hammerhead ribozyme.
- Objective 2: To monitor the progress of this reaction using a toehold mediated strand displacement reaction on the same DMF chip and in an automated fashion.
- Objective 3: To compare the results of ribozyme reactions on the DMF chip to that on a well-plate. Thereby to study how efficiently the ribozyme cleaves in the experiments on DMF chips when compared to well-plate experiments.

The remainder of the thesis will demonstrate that we were successful in achieving all the objectives. The results from the study indicate that there are significant potential and actual advantages in applying DMF technology to the performance of ribozymatic experiments, opening the door for possible synthetic biology and computational biology applications.

Chapter 2: Experimentation and Methodology

2.1 Benchtop experiments

2.1.1 Ribozyme assembly and transcription

Ribozymes were transcribed from a DNA template (Figure 8) produced by carrying out an assembly PCR of overlapping primers. The primers F1, F2, R1 and R2 (Table 1) for the ribozyme were generated using the tool Primerize [81]. A PCR reaction mixture composed of primers F1 (2 μM), R1 (0.2 μM), F2 (0.2 μM), R2 (2 μM), Taq polymerase (hotStar Taq Plus from QIAGEN) with its reaction buffer at 1x, Q-solution (1x from QIAGEN), 0.2 mM of dNTPs (DGel electrosystem) and milli-Q water, was prepared at a fixed volume of 100 μL . The reaction mixture was denatured at 95°C for 15 min and subjected to 15 cycles of 30 sec denaturation at 95°C, 30 sec annealing at 50°C, and 30 sec extension at 72°C. Finally, the PCR product was ethanol precipitated.



Figure 8: Schematic representation of Primerize assembly design.

Primer Name	Primer Sequence
R1	5' CGTCCGAAGGGTGAGAAATCGCAGAGCCTACATGTCCGACTCAT 3'
F1	5' TTCTAATACGACTCACTATAGGAAATCCCTGATGAGTCCGACATGTAGGCT 3'
R2	5' ACAGGGTCGGACCTGGAAATCCTACGCAGGCGTGC GTT 3'
F2	5' TCTCACCTTCGGACGAAACGCACGCCTGCGTAGGATTCCA 3'

Table 1: Primers are generated by the tool Primerize for the assembly of the ribozyme.

For 1 mL *in vitro* RNA synthesis reaction, 10 PCR reactions (100 μ L each) were mixed, precipitated, and resuspended in 150 μ L milli-Q water. The reaction mixture for *in vitro* RNA synthesis contained 80 mM HEPES (pH 7.5), 24 mM MgCl₂, 40 mM dithiothreitol, 2 mM spermidine, 6 μ g/mL T7 polymerase, the 150 μ L of resuspended PCR product (10 reactions), 2 mM rNTPs, 1x pyrophosphatase (Roche diagnostics) and 200 U (40 μ L) RiboLock (Thermo Fisher Scientific). The mixture was incubated for 30 min at 37°C. Immediately after, the mixture was treated with 10 U of DNase (New England Biolabs) and left for incubation at 37°C for 30 min. After extracting the RNA using phenol-chloroform, the aqueous phase was ethanol precipitated. Purification of the RNA was done in 10% denaturing (8 M urea) polyacrylamide gel and UV-shadowing was used to visualize bands. The largest band on the gel (as there was some level of cleavage during transcription) was cut out and eluted in 0.3 M NaCl overnight at 4°C. The eluent was ethanol precipitated and resuspended in nuclease-free water.

2.1.2 Preparation of probe

A probe for detecting ribozyme self-cleavage consisted of two single-stranded DNA (ssDNA) molecules, namely an F-strand and a Q-strand (Figure 9). The 5' end of the F-strand was linked to

a fluorophore (Cy5) while a Black Hole Quencher (BHQ-3) was attached to the 3' end of the Q-strand. The two strands were purchased from Alpha DNA (Montreal, Canada).

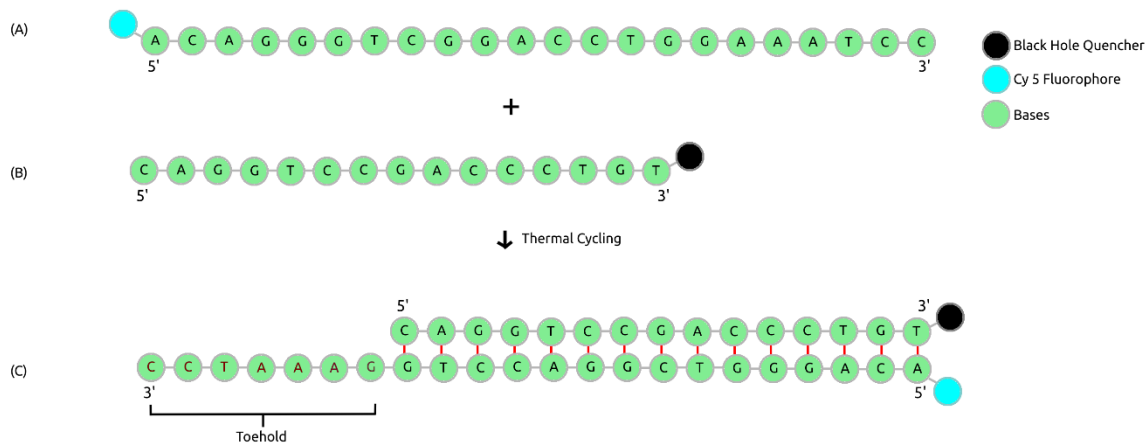


Figure 9: Preparation of the quenched probe.

(A) A single-stranded DNA (ssDNA) with a Cy5 fluorophore linked to its 5'-end (named F-strand). (B) An ssDNA with a black hole quencher (BHQ-3) attached to its 3'-end (Q-strand). A mixture of F-strand ($0.6 \mu\text{M}$) and Q-strand ($0.6 \mu\text{M}$) in the cleavage-buffer yields a quenched probe (C) after thermal cycling (3 min denaturation at 95°C , 15 min annealing at 50°C , and annealing at 37°C for 15 minutes). The quenched probe has seven unbounded bases (indicated in red) at the 3' end of the bottom strand forming a toehold. When the probe is mixed with a strand (ssDNA or RNA) complementary to the F-strand, the toehold facilitates a stronger binding between the newly added strand and F-strand. This displaces the quencher from the probe and allowing it to fluoresce.

The pre-annealed quenched probe was prepared in a 1.25x cleavage buffer (125 mM NaCl, 62.5 mM tris-HCl pH 7.5, 31.25 mM KCl) with F-strand ($0.625 \mu\text{M}$) and Q-strand ($0.7 \mu\text{M}$). The mixture was incubated in a thermocycler (Biorad T100), 3 min denaturation at 95°C , 15 min annealing at 50°C and 15 min annealing at 37°C . The final mixture was prepared in bulk and stored at -20°C . Before usage, a solution of surfactant Tetric® 304 (Sigma-Aldrich) (0.05% per $10 \mu\text{L}$) was also added to the mixture.

2.1.3 Benchtop ribozyme cleavage assay

In a black-sided flat clear-bottom 384 well plate, 2 μL of the ribozyme (2.5 μM) was mixed with 8 μL of cleavage-buffer (1.25x) containing 6.25 μM input ssDNA and 12.5 mM MgCl_2 . In addition, five wells near the assayed wells were filled with 30 μL water to maintain the humidity within the well-plate. The plate was then covered with its lid and sealed using parafilm. The well-plate was inserted into a microplate reader ClarioSTAR® (BMG Labtech) to take fluorescence readings every 20 min with 8 flashes at $\lambda_{\text{ex}} = 647$ nm, $\lambda_{\text{em}} = 665$ nm, at 37°C. The focal length and gain for the measurements were calibrated using a 10 μL solution of 0.5 μM fluorophore (Cy5) and was set to 6.4 mm and 1800, respectively.

2.2 DMF chip experiments

2.2.1 DMF chip fabrication

A standard photolithography method, as previously reported [76], was used for fabrication of the digital microfluidics devices. A photomask was designed in AutoCAD 2018 (AutoDesk™) and printed on transparency film (CAD/Art services, Bandon, OR). A glass substrate pre-coated with S1811 photoresist (Telic) was exposed to UV (8 sec) under the photomask on a Quintel Q-4000 mask aligner (Neutronix Quintel). Substrates were developed using MF321 developer (Rohm and Haas), baked (115°C, 1 min) and etched in CR-4 chromium etchant (OM Group). The remaining photoresist was stripped using an AZ-300T stripper (2 min). After rinsing with deionized (DI) water and air drying, the substrates were silanized (DI water, 2-propanol, (trimethoxysilyl) - propyl methacrylate, 50:50:1) for 15 min.

Electrode contact pads were covered with Kapton tape (Kapton®), after which a dielectric, 7 μM Parylene-C (Specialty Coating Systems) was deposited on the substrates using an SCS Labcoter 2 PDS 2010 (Specialty Coating Systems). Finally, a top plate was cut to size from an ITO (indium tin oxide) pre-coated glass slide (cat no. CG-61IN-S207, Delta Technologies). A hydrophobic layer of 1% Teflon-AF (FC40) was deposited on both the bottom substrate and the top plate, using a Laurell spin coater (North Wales) (500 rpm, 100rpm/sec, 30 sec; 3000 rpm, 500 rpm/sec, 60 sec), after which the substrates were baked (160°C, 10 min). The device was assembled by placing small stacks of 2 layers of double-sided tape (3M Canada) (each of thickness - 70 μm) in between the bottom and top plates (Figure 10).

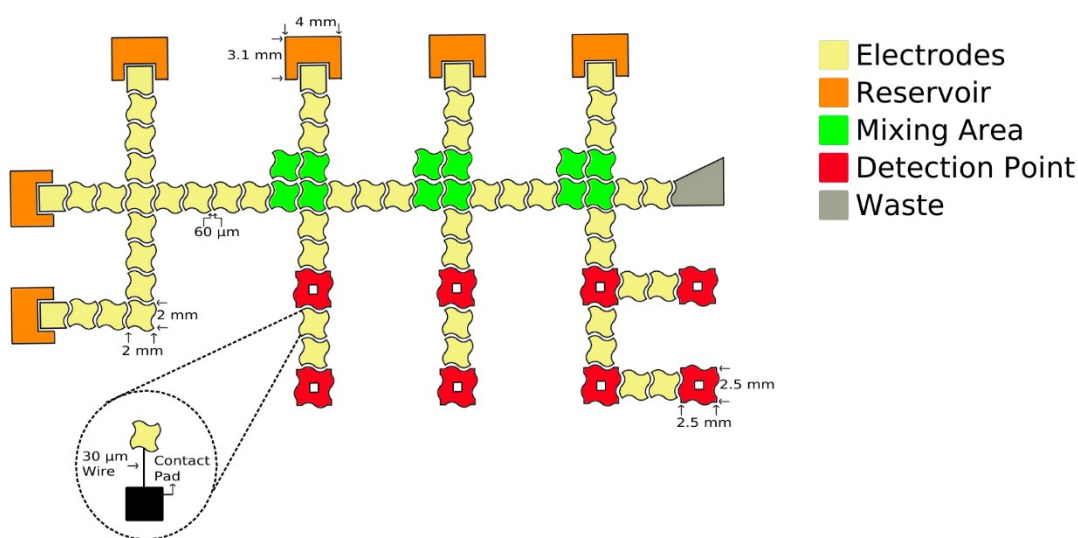


Figure 10: A schematic of the DMF chip and device operations.

The design consists of 64 electrodes ($2 \times 2 \text{ mm}^2$ each), 6 reservoirs ($4 \times 3.1 \text{ mm}^2$ each), 3 mixing areas (composed of 4 electrodes each) and 8 detection points ($2.5 \times 2.5 \text{ mm}^2$ each). The inter-electrode spacing in the design is maintained 60 μm . The electrodes are connected to the contact pad using connecting wires of thickness μm .

2.2.2 Automation system for the DMF chip

The automation system was composed of in-house Python 2.7 software [82] to control an Arduino Uno microcontroller (Adafruit) driven control board. A 15 kHz sine wave output from a function generator (Agilent Technologies) was amplified by a PZD-700A amplifier (Trek Inc.). The amplified signal was used as the driving input with a voltage of 178 V (V_{RMS}), which was delivered to a control board that passed it on to the electrode, bypassing high-voltage optocouplers on the control boards. An I/O expander (Maxim 7300, Digikey) controlled the logic state of each solid-state switch (high or pulled-to-ground) through I2C communication. The control board was interfaced with pogo pins, where the switches deliver high-voltage potential (or ground) to the contact pads on the chip. The top plate of the device was grounded. The hardware assembly and instructions to install the open-source codes are detailed on the Shih lab repository (available on request).

The droplets on the chip were driven by actuating the electrodes. A voltage of V_{RMS} (178 V) was applied to switch the electrodes ON. The protocol file associated with the automation system was updated with the parameters for each sequential actuation of electrodes, required by the automation system. Each sequence can be further configured (electrode pulse time and period) and can be initiated through the command line.

2.2.3 DMF chip ribozyme cleavage assay

The DMF substrate was cleaned up using RNase away, IPA, DI water, and subsequently air-dried. After mounting the device onto the automation system, 2.5 μL of the ribozyme (2.5 μM) and 2 μL of cleavage buffer (1.25x) were pipetted onto the reservoirs and detection points, respectively. The top plate was then placed on the chip and was connected to a ground wire. A droplet of ribozyme

($\sim 0.5 \mu\text{L}$) was dispensed from the reservoirs, using a dispense electrode pattern, to the third electrode. This droplet was then moved towards the detection point by sequentially actuating four electrodes between the electrode with the dispensed droplet and the detection point. The droplet containing ribozyme was then merged with the droplet of cleavage buffer at the detection point. The resulting droplet was moved up and down across the detection point by actuating four electrodes for 10 sec to mix all the droplet contents.

After merging and mixing the droplets, the chip was carefully removed from the automation system and stacked on a Corning® 384 well-plate (black and flat bottom). The detection points were aligned to the wells in the well-plate, and the wells surrounding the chip were filled with $30 \mu\text{L}$ of water. The well-plate was then covered with its lid and sealed using parafilm. This setup was inserted into a plate reader ClarioSTAR® (BMG Labtech) to measure fluorescence. Wells aligned to the detection points were scanned using a well-scanning program in the plate reader via a scan matrix (30×30 pixels, where each pixel represented 10 mm^2). The well-scans were taken regularly every 20 min at 37°C , with 8 flashes, a focal height of 15.80 mm and a gain of 1800 ($\lambda_{\text{ex}} = 647 \text{ nm}$, $\lambda_{\text{em}} = 665 \text{ nm}$). From the scanned matrix, the region corresponding to the detection point was selected and the fluorescence was noted.

Chapter 3: Results and Discussion

3.1 DMF chip design and architecture

Digital Microfluidics (DMF) platforms have found their application in automating a variety of enzymatic reactions [45], [45], [53], [70] and were monitored using luminescence [83] and fluorescence [70]. Ribozyme cleavage reactions are one type of such enzymatic reactions [84] and can similarly be analyzed by reading fluorescence intensities [29], [85]. In this work, we designed a digital microfluidics chip to carry out a cleavage reaction of an inducible *cis*-acting hammerhead ribozyme (HHR). The chip also served as a platform to monitor ribozyme cleavage by recording the fluorescence intensity of a quenched probe, where the cleaved RNA strand binds to the probe displacing the quencher, allowing the probe to fluoresce.

The chip was designed to carry out six ribozymatic reactions and two control reactions on the same chip, by merging ribozyme-containing droplets with droplets of cleavage buffer and quenched probe (Figure 11). For this reason, the design had six reservoirs for dispensing droplets containing ribozyme and cleavage buffer. The device also had eight detection areas to isolate and monitor the six assayed droplets along with the two controls- a negative and a positive control. In addition to this, three mixing areas composed of four electrodes were included in the chip. The inter-electrode spacing ($60\ \mu\text{m}$) was made to be twice the thickness of wiring ($30\ \mu\text{m}$) because some of the inner electrodes were connected to the contact pads through the spacing between the electrodes (Figure 10). Moreover, the electrode edges were shaped as ‘skewed-waves’, which facilitated successful droplet movements across the DMF device. Studies have confirmed that square or rectangular shaped electrodes often cause droplets to be stranded, ceasing droplet motion on the chip [86]. Comb, zig-zagged or crescent shapes are also said to have solved the problem

[87], [88]. However, regions with pointy edges and high electric fields (>108 V/cm) are known to cause a dielectric breakdown [89], while ‘skewed-wave’ edged electrodes have been proven to resolve this problem [71].

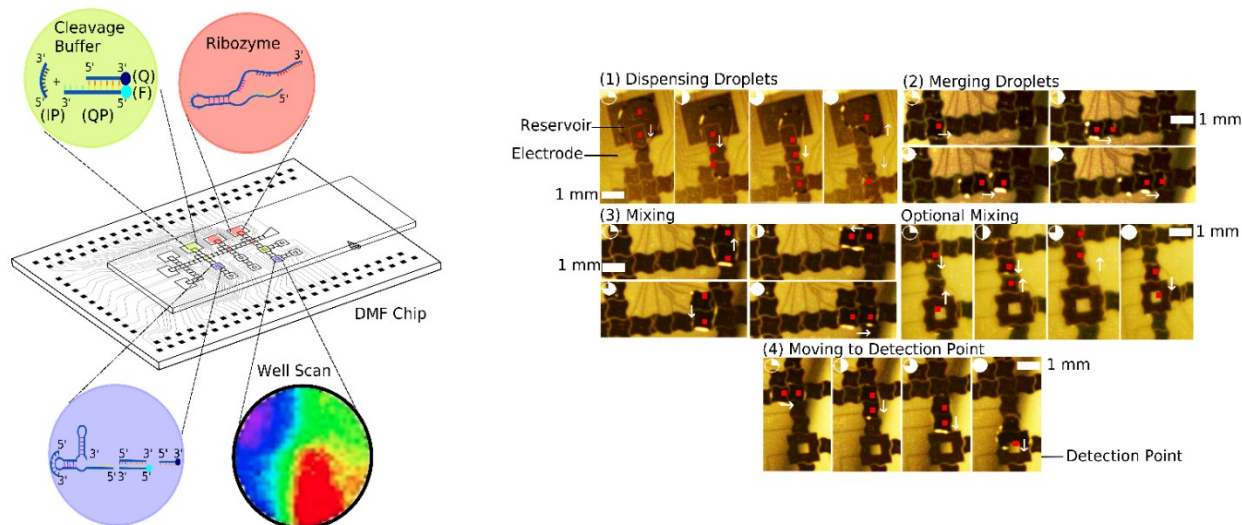


Figure 11: Overview of the ribozyme cleavage assay on a digital microfluidic (DMF) chip.

On the DMF device, the ribozyme cleavage experiment is carried out in four steps, which are depicted in screenshots of different frames, from a video of the experiment, where the red dots indicate the electrodes actuated in each frame. (1) First, a ribozyme-containing droplet ($0.625 \mu\text{M}$) and another containing cleavage buffer ($1.25\times$) are dispensed from their respective reservoirs by splitting (15 kHz, 178 V_{rms}). The ribozyme used in the experiment is an inducible cis-acting hammerhead ribozyme (HHR). The cleavage buffer contained $6.25 \mu\text{M}$ input strand (IP, a ssDNA to activate the ribozyme) and a quenched probe (QP) comprising of two ssDNA strands, one with Cy5 fluorophore (F) and the other with a black hole quencher (Q). (2) Next, the dispensed droplets are moved closer to each other and then merged. (3) The merged droplets are mixed by actuating four electrodes, to move the droplets in a loop three times. (4) Finally, the assayed droplet is driven to the detection point for measurement. Optionally, the experiment can also be carried out by merging a dispensed ribozyme-containing droplet with an already pipetted droplet of cleavage buffer at the detection point. The merged droplet can then be mixed by moving it back and forth across the detection point three times. In the assayed droplet, the ribozyme cleaves itself after folding into an active hammerhead ribozyme (HHR), upon binding to the input strand. The cleaved-off RNA strand binds to the probe displacing the quencher, allowing the probe to fluoresce. Hence, measuring the fluorescence intensity reflects the amount of cleaved-off RNA strand that actually detaches from the ribozyme. The fluorescence of the assay is read by well-scanning the DMF device using a plate reader.

Droplet motion on the chip was achieved by actuating the electrodes for 0.7 sec at a voltage of 178 V (15 kHz sine wave). In order to dispense droplets, a larger droplet was initially stretched by actuating four electrodes from the reservoir. After that, the third electrode was switched off, forcing a small droplet to separate from the larger droplet (Figure 11). When 2.5 μL of reagent was pipetted on to the reservoir, the actuation of electrodes (surface area = 4 mm²) dispensed droplets of the size of 0.5 +/- 0.08 μL (n = 10). The dispensed droplets were merged and mixed at the mixing area by activating four electrodes in loops, three times (Figure 11).

During preliminary experimentation, ribozyme-containing droplets were moved across the chip and were reproducible without damaging the electrodes. However, the cleavage buffer droplets, which also contained the input ssDNA and the quenched probe, often failed to move across the chip and sometimes burned the electrodes, indicating greater biofouling. Studies have shown that droplets with high alkaline content often caused significant biofouling [70], which could be the same for the cleavage buffer droplet, as it contains high salt content. Adding surfactants to such solutions have proven to be effective, even without any filler oil. Hence 0.05% Tetric® 304 was added to the aqueous cleavage buffer. Though the surfactant resulted in improved movement of the cleavage buffer droplets, it was observed that the droplets had left traces along their paths, which made chip reuse quite difficult. Therefore, the reactions were done at a larger volume (2.5 μL), by directly dispensing cleavage buffer droplets on to the detection points and then merging them with ribozyme-containing droplets. Hence, the droplets were successfully mixed by moving them back and forth three times across the detection points, which required activation of six electrodes. However, moving the final droplet still caused biofouling and therefore, for the later experiments, while mixing, the number of electrodes was limited to four, and the droplets were moved back and forth the detection points only thrice (Figure 11).

In order to measure fluorescence intensities, a previously established protocol [71], [72] was followed. After executing the experiments on the DMF chip, the device was carefully removed from the automation system, and placed on a flat black-sided clear-bottom 384 well-plate, while carefully aligning the detection points with the wells. Five wells around the chip were filled with 30 μL of DI water to reduce evaporation, because the DMF chip fluorescence intensities of all the assays, including the controls, were found to increase significantly after 60 min. Previous experiments [90], [91] have used filler oil to prevent DMF chip droplet evaporation, but this can cause the probe to leak into the oil, resulting in cross-contamination [65]. The well-plate was covered by a lid and sealed using parafilm, then scanned in a plate reader (ClarioSTAR®) at 37°C. The machine takes up to 20 min to scan the entire chip. Thus, readings correspond to fluorescence intensities at 20 min intervals, starting from the moment the well-plate is placed in the plate reader. From the resultant matrix of pixels (Figure 12A), the regions corresponding to the detection points were selected, and the highest fluorescence intensity of each detection point was recorded. After 180 minutes, the positive control, a strand displacement reaction, exhibited an average highest fluorescence reading of 12250 units (Figure 12B). The assayed ribozyme reported a fluorescence intensity of 4900 units, while a low fluorescence level of 1530 units was recorded for the negative control (a quenched probe).

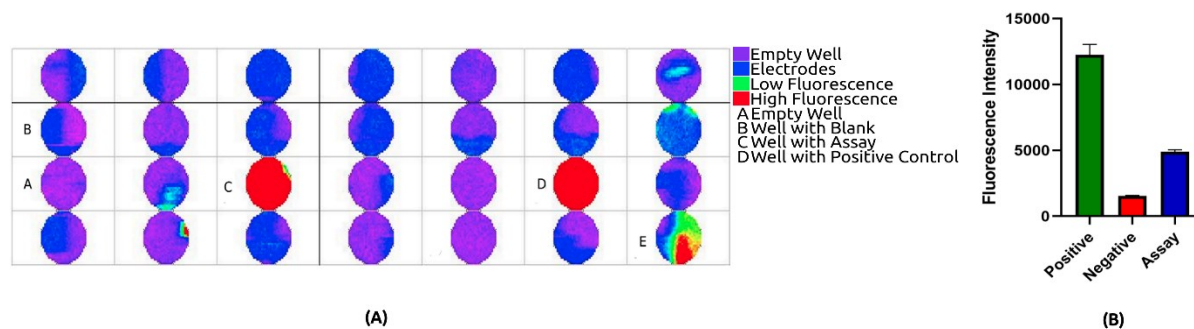


Figure 12: On-chip fluorescence intensity measurements.

(A) A well-scan of the DMF device after carrying out a ribozymatic experiment (chip is scanned after 180 mins). The droplets of the ribozyme cleavage assay and positive control (a strand displacement reaction) exhibit high fluorescence, whereas the negative control (a quenched probe) displays a low fluorescence. (C) A plot of the highest fluorescence intensities at the detection points corresponding to each droplet ($SD = \pm 1$).

The results demonstrated that the designed DMF chip could manipulate the droplets containing ribozymes and the cleavage buffer with no or minimal biofouling. In this way, the ribozyme cleavage reaction could be initiated on the DMF by merging and mixing the ribozyme and buffer droplets. Moreover, the progress of the reaction could also be monitored by the fluorescence.

3.2 Benchtop and DMF chip monitoring of ribozyme cleavage kinetics

The research primarily aims to demonstrate the feasibility of performing ribozyme cleavage experiments on DMF platforms. To achieve this, a cleavage assay using an inducible *cis*-acting hammerhead ribozyme (HHR) was carried out both in well-plate and on a DMF chip, and the results were compared. The cleavage was then monitored by reading a fluorescent signal generated by the probe, once the quencher has been displaced by the ribozyme's output strand.

The well-plate and DMF chip experiments were performed following the same workflow as detailed in chapter 2, after which the fluorescence intensities were read regularly every 20 min.

In addition to the cleavage assay, the experiments had a positive control (a strand displacement reaction), and a negative control (quenched probe).

The fluorescence intensities of both the well-plate and DMF chip experiments were plotted against time (Figure 13). The change in fluorescence intensities over time was then analyzed by fitting a line to the readings using linear regression (Figure 14). The line fit to the readings from the positive control (PC) both in the well-plate, and on the chip had smaller slopes (Student t-test, $P > 0.05$, $P^{\text{PC}}_{\text{Well-Plate}} = 0.78$, $P^{\text{PC}}_{\text{DMF}} = 0.78$) indicating no or a small change in fluorescence during the experimentation ($\text{Slope}^{\text{PC}}_{\text{Well-Plate}} = -1 \pm 3.5$, $\text{Slope}^{\text{PC}}_{\text{DMF}} = 0.85 \pm 3.1$). Similarly, a small change in the fluorescence intensities (Student t-test, $P > 0.05$, $P^{\text{NC}}_{\text{Well-Plate}} = 0.3$, $P^{\text{NC}}_{\text{DMF}} = 0.08$) was observed for the negative controls (NC) in the well-plate and on the chip with smaller slopes ($\text{Slope}^{\text{NC}}_{\text{Well-Plate}} = 0.53 \pm 0.51$, $\text{Slope}^{\text{NC}}_{\text{DMF}} = 0.33 \pm 0.18$). Whereas the line fit to the assayed ribozyme (RZ) had a positive slope (Student t-test, $P < 0.05$, $P^{\text{RZ}}_{\text{Well-Plate}} < 0.0001$, $P^{\text{RZ}}_{\text{DMF}} < 0.0001$) both on the chip and well-plate, indicating an increase in the fluorescence intensities over time on these platforms ($\text{Slope}^{\text{AS}}_{\text{Well-Plate}} = 10.30 \pm 1.6$, $\text{Slope}^{\text{AS}}_{\text{DMF}} = 11.2 \pm 0.8$). This rise in fluorescence indicated that, in presence of the inducing DNA strand, the HHR folded into an active ribozyme, leading to self-cleavage. Hence, the cleaved-off RNA strand displaced the quenching strand and hybridized to the probe, allowing the probe to fluoresce, in both the DMF chip and the well-plate. Both well-plate and chip assays displayed similar trends over time. The results show no significant difference between the two assays (Student t-test, $P > 0.05$, $P^{\text{AS}}_{\text{DMF_Vs_Well-Plate}} = 0.054$). This provides good evidence that the ribozyme cleavage experiment was reproducible on the DMF chip. Moreover, we noticed that the assay readings from the DMF chip exhibited a smaller standard deviation than that of the well-plate experiments (Student t-test, $P > 0.05$, $P^{\text{SD}}_{\text{DMF_Vs_Well-Plate}} = 0.0054$). The errors in well-plate assays could have been introduced due to

pipetting and other human errors, which are minimized on a DMF platform. This was verified by measuring the signal-to-noise ratio (SNR) for both DMF chip and well-plate readings. The signal-to-noise ratio (SNR) was calculated by dividing the arithmetic mean of the fluorescence readings of the triplicates for each assay by their standard deviation. At the end of 180 min, the fluorescence readings of the assay on the DMF chip exhibited an improved SNR compared to the well-plate readings ($\text{SNR}_{\text{Well-Plate}} = 8.95$, and $\text{SNR}_{\text{DMF}} = 18.95$, Student P-test, $P < 0.05$, $P_{\text{SNR}} = 0.0023$). These calculations showed that DMF technology can provide more reliable platforms to execute ribozymatic assays- a property that was also observed in previous studies [70].

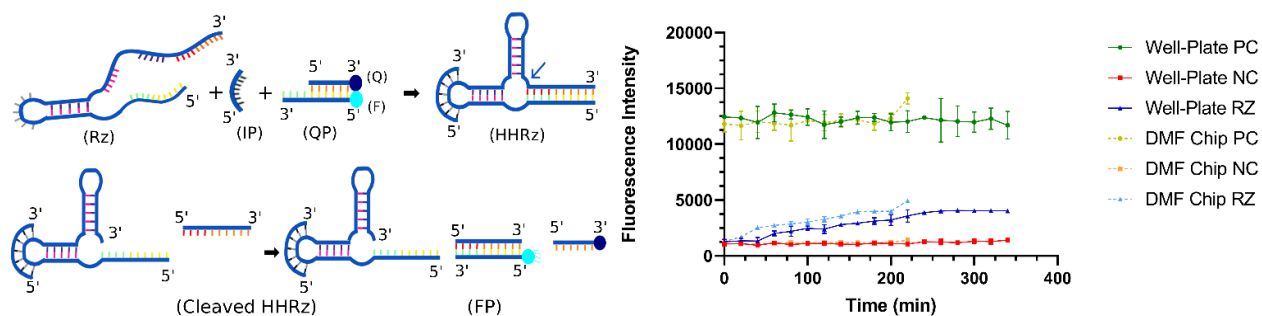


Figure 13: Comparison of the ribozyme well-plate and DMF chip assay.

Monitoring cleavage of the ribozyme was done by reading the fluorescence intensities resulting from the experiments performed in a well-plate and DMF chip. In the experiments, a solution (or droplet) of the ribozyme ($0.5 \mu\text{M}$) is mixed with a solution containing cleavage buffer with a single-stranded DNA input (IP) ($5 \mu\text{M}$) and a quenched probe ($0.5 \mu\text{M}$). The input strand (IP) binds to the ribozyme inducing it to fold into an active hammerhead ribozyme (HHR). In the active state, the ribozyme cuts-itself at a position indicated by the arrow. The small RNA strand (output strand) that leaves the ribozyme after cleavage displaces the quencher and binds to the probe, rendering it fluorescent. The fluorescence intensities are read every 20 min and plotted against time. This shows the amount of output strand that leaves the ribozyme and binds to the probe, over time. The continuous and dotted lines correspond to the experiments in the well-plate and on the chip, respectively. In addition to the ribozyme assay (RZ), the experiments had positive (PC) and negative controls (NC). For NC a quenched probe ($0.5 \mu\text{M}$) is used. For PC a strand displacement reaction using a ssDNA strand ($0.5 \mu\text{M}$) equivalent to the expected cleaved-off output RNA strand is used to displace the quencher from the probe.

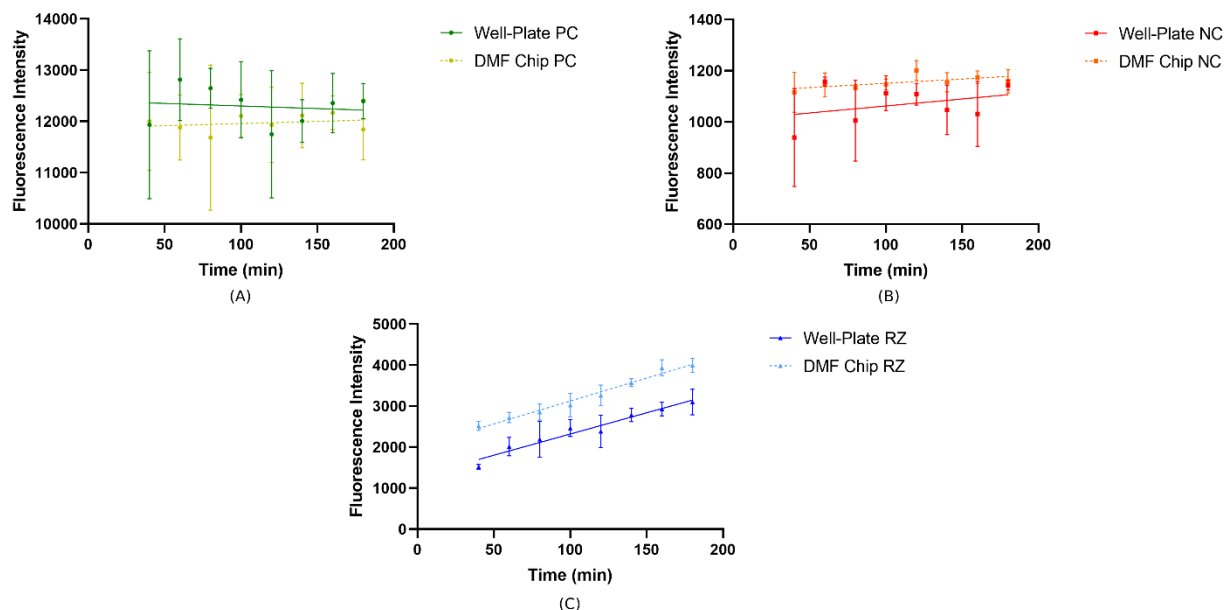


Figure 14: Analysis of change in fluorescence in the ribozyme cleavage experiment.

The ribozymatic assay (AS) with one positive control (PC, a strand displacement reaction) and negative control (NC, a quenched probe) is carried both on a DMF chip and well-plate. The fluorescence intensities are read every 20 min and were plotted against time. A straight line is fit to the readings between 40 min and 180 min (linear region) using linear regression to analyze the change in fluorescence over time. The slopes of the lines indicated the change in fluorescence as time progressed. (A) The lines fit to the positive controls exhibit a low slope indicating no or minimal increase in fluorescence both on the chip and well-plate. (B) The negative controls on both platforms display a negligible change in the fluorescence intensities as indicated by the lines with a low value of slopes. (C) The lines fit to the readings from the on-chip, and benchtop assays are steeper indicating an increase in fluorescence intensities due to the cleavage of the ribozyme over time.

Parameters	Well-Plate	DMF Chip
YIntercept	1000 +/- 61	1120 +/- 22
XIntercept	-1840 +/- 550	-3300 +/- 1500
Slope	0.53 +/- 0.51	0.33 +/- 0.18

Table 2: Parameters of linear regression fit to the benchtop and DMF chip negative controls.

Parameters	Well-Plate	DMF Chip
YIntercept	12400 +/- 420	11900 +/- 360
XIntercept	12500 +/- 1580	-14000 +/- 1560
Slope	-1.0 +/- 3.5	0.85 +/- 3.1

Table 3: Parameters of linear regression fit to the benchtop and DMF chip positive controls.

Parameters	Well-Plate	DMF Chip
YIntercept	1290 +/- 140	2010 +/- 95
XIntercept	-120 +/- 40	-180 +/- 40
Slope	10.30 +/- 1.6	11.2 +/- 0.8

Table 4: Parameters of linear regression fit to the benchtop and DMF chip assay.

The inverse of fluorescence intensities from the readings can also help us determine the decay of uncleaved ribozyme over time, providing insight into ribozyme kinetics. The ribozyme was consumed during the reaction, and hence the rate of reaction was calculated from the amount of uncleaved ribozyme at different time points according to a first-order reaction [92]. Therefore, the kinetics of ribozyme cleavage can be analyzed using a one-phase decay equation [11] (Figure 15). The inverse of fluorescence intensities was plotted against the time and fitted with a one-phase decay equation ($R^2_{\text{Well-Plate}} = 0.84$ and $R^2_{\text{DMF}} = 0.95$) (Figure 10). The reactions proceeded at a rate, $k_{\text{obs}}^{\text{Well-Plate}} = 0.01 \pm 0.003 \text{ min}^{-1}$ in the well-plate and $k_{\text{obs}}^{\text{DMF}} = 0.026 \pm 0.005 \text{ min}^{-1}$ on the chip. Eventually, the amount of uncleaved ribozyme reached a plateau (Table 5).

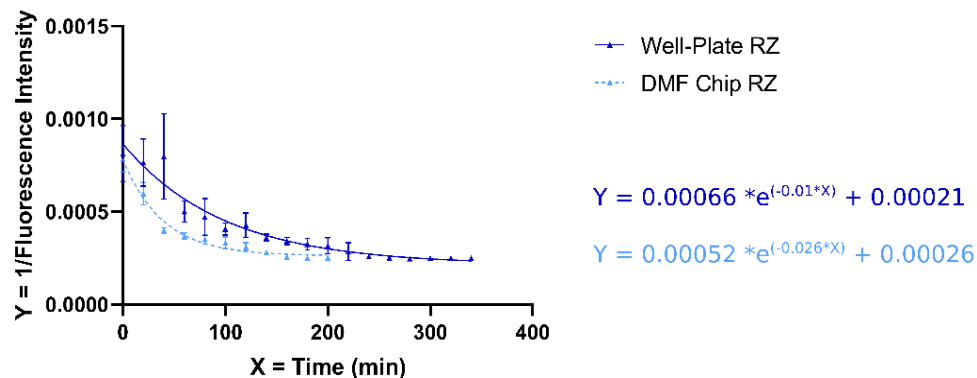


Figure 15: Well-Plate and DMF chip kinetics of the ribozyme cleavage assay.

The inverse of fluorescence intensities of the ribozyme cleavage assay (AS) was plotted against time to express the fluorescence readings as a decaying function of the uncleaved ribozyme. The change in the fluorescence intensities over time is expressed as a one phase decay equation of the form, $Y = (Y_0 - \text{Plateau}) * e^{-KX} + \text{Plateau}$; Y = the amount of uncleaved ribozyme, X = time in min, K = rate of the reaction, Y_0 = initial value of Y , and Plateau = the value of Y at which the reaction reaches a plateau.

Parameters	Well-Plate	DMF Chip
Y_0	0.00087 +/- 0.00007	0.00078 +/- 0.00004
Plateau	0.00021 +/- 0.00008	0.00026 +/- 0.00002
K	0.01 +/- 0.003	0.026 +/- 0.005
Half Life	68 +/- 18	27 +/- 5
Tau	99 +/- 25	39 +/- 7.3
Parameters	Well-Plate	DMF Chip

Table 5: Parameters of one phase decay regression fit to the benchtop and DMF chip ribozyme cleavage assay.

Interestingly, it was also observed that the rate of cleavage of the ribozyme on the DMF chip, $k_{\text{obs}}^{\text{DMF}}$ (0.026 +/- 0.005 min⁻¹) was ~ 2.5 times that of the well-plate cleavage rate, $k_{\text{obs}}^{\text{Well-Plate}}$ (0.01 +/- 0.003 min⁻¹). It was hypothesized that this was due to the higher surface area to volume (SAV) ratio of reaction-holding droplets in the DMF platform. The increased SAV can lead to

improved intermolecular collisions, thereby increasing the rate of reaction [44], [93]. The higher rate of cleavage could have also been due to molecular crowding, caused by surfactant molecules (Tetronic® 304), as discussed in other studies [94].

The results from the above experiments demonstrated the successful deployment of ribozyme cleavage experiments on a DMF chip. DMF is a promising technology that could provide platforms to carry out such ribozymatic experiments in an automated fashion, at a higher rate and using lower volumes of reagents, leading to a significant reduction in experimental costs.

3.3 Benchtop and DMF chip analysis of ribozyme as a biosensor

Ribozymes have found their applications as biosensors for the detection of a variety of organic molecules including antibiotics, specific nucleic acid sequences, peptides, proteins, and metal ions [25], [26], [28], [95]. In our own experiment, a ribozyme was used to detect the concentration of input DNA strands. Here, we show that a DMF protocol can facilitate an experiment to validate the sensitivity and limit of detection of a ribozyme-based DNA biosensor.

Ribozyme cleavage experiments were performed both on the DMF chip and well-plate at different input concentrations (10 μM , 5 μM , 1 μM , 0.75 μM , 0.5 μM , 0.25 μM , 0.1 μM , 0.01 and no input) following the protocols described in chapter 2. For each input concentration, the fluorescence intensities were recorded every 20 min, for a total period of 180 min, showing the progress of cleavage over time (Figure 16).

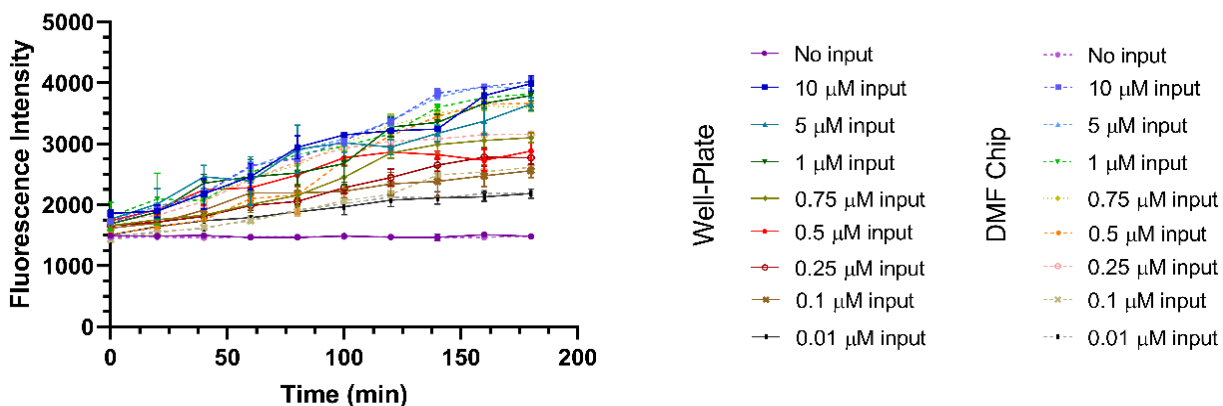


Figure 16: Monitoring the progress of ribozyme cleavage reactions with varying input concentrations.

At first, the ribozyme cleavage assays are performed both on the DMF chip and well-plate at different input ssDNA concentrations (10 μM , 5 μM , 1 μM , 0.5 μM , 0.25 μM , 0.1 μM , 0.01 μM and zero input). Then fluorescence intensities are recorded every 20 min and plotted against time for 180 min to observe the progress of the cleavage reaction.

To examine the sensitivity of the ribozyme as a sensor, a calibration (or standard) curve was generated by plotting the endpoint (180 min) fluorescence readings for each assay against the input concentration on a logarithmic scale (Figure 17). These results from both the chip and well-plate assays followed a sigmoidal curve (Table 6). Next, a linear regression model was fit to a near-linear region (between 0.1 μM and 1 μM) of the sigmoidal curve. As shown in previous studies, the slope of the fitted line indicated the sensitivity of the biosensor [96]. The fitted lines for both the chip and well-plate displayed a positive slope ($\text{Slope}^{\text{RzB}}_{\text{Well-Plate}} = 850 \pm 120$ and $\text{Slope}^{\text{RzB}}_{\text{DMF}} = 1230 \pm 71$). However, the line fitted to the readings from the chip had a steeper slope and smaller standard error showing a higher sensitivity on the DMF platform than in the well-plate (Student t-test, $P < 0.05$, P-value = 0.0087). The higher sensitivity on the DMF chip could be due to the high SAV ratio of reaction-holding droplets on the DMF platform [44], [93].

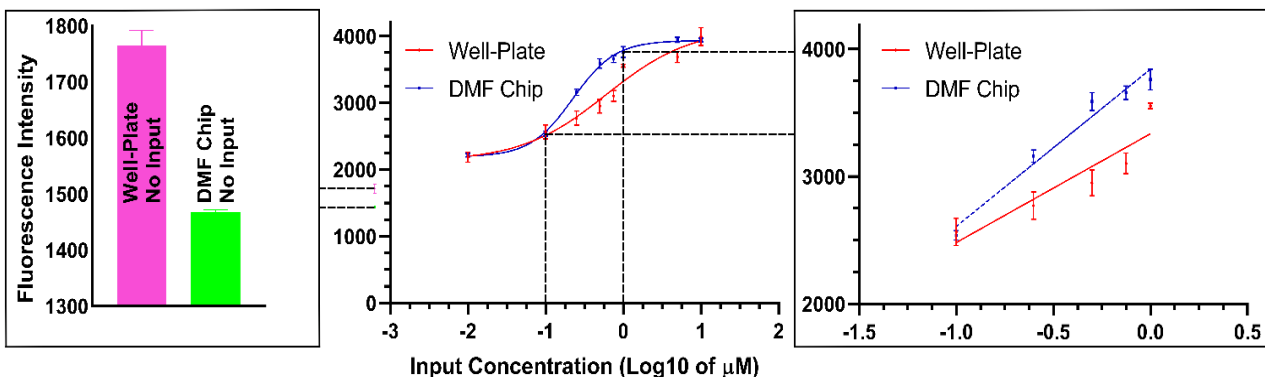


Figure 17: Analysis of ribozyme as a biosensor by activating the ribozyme with varying input concentrations.

After carrying out the ribozyme cleavage assays at different input concentrations, the endpoint (180 min) fluorescence readings of each assay are noted and plotted as a function of input concentration (in Log10 scale). A four-parameter logistic (4-PL) sigmoidal model is fit to the graph, from which a near-linear region is extracted for further analysis (between 0.1 μM and 1 μM). A linear regression model is fit to the extracted region and used to calculate the sensitivity and limit of detection of the ribozyme, as a sensor of an input ssDNA strand. Additionally, the endpoint fluorescence intensities of the assays without input are also measured to calculate the limit of quantification of the ribozyme.

Parameters	Well-Plate	DMF Chip
Top	4100 +/- 300	3900 +/- 50
Bottom	2100 +/- 250	2100 +/- 70
LogIC50	-0.22 +/- 0.21	-0.6482 +/- 0.2
IC50	0.61 +/- 0.31	0.22 +/- 0.02
Parameters	Well-Plate	DMF Chip

Table 6: Parameters of sigmoidal curve fit to the ribozyme cleavage assay on benchtop and DMF chip experiments with different input concentrations.

In addition, parameters of the ribozyme-based biosensor, such as limit of detection (LoD) and limit of quantification (LoQ) were calculated. These parameters further characterize the ribozyme as a biosensor [96], [97]. LoD indicates the lowest input concentration in the assay at

which the detection can be differentiated from an assay with no input. Whereas LoQ represents the concentration level of the input above which the quantitative results can be presented with confidence. LoD and LoQ were calculated using equations $\text{blank}_{\text{mean}} + 3 * \text{SD}$ and $10 * \text{SD}/S$ respectively, where $\text{blank}_{\text{mean}}$ is the mean fluorescence intensity of assays with no input ssDNA, SD is the standard deviation of the $\text{blank}_{\text{mean}}$ and S is the slope of the regression line[98], [99]. The LoD of the experiments on the chip was observed to be ~80% of that in the well-plate ($\text{LoD}_{\text{Well-plate}} = 1845$, $\text{LoD}_{\text{DMF}} = 1475$). Similarly, the LoQ of the experiments on the chip was ~8% of that in well-plate assays ($\text{LoQ}_{\text{Well-Plate}} = 0.31$ and $\text{LoQ}_{\text{DMF}} = 0.025$). These low LoD_{DMF} and LoQ_{DMF} values showed that the ribozyme performs better as a biosensor on the DMF chip than in the well-plate. The improvements to the detection limits of the ribozyme-based biosensor could also be due to the higher SAV ratios on DMF chips, also recorded in prior research involving microfluidic platforms [100].

The above results demonstrated that the near-linear sections of the standard curves generated from the cleavage assays on the DMF chip and well-plate could be used to characterize ribozymes. These readings could also be utilized to describe the activity of ribozyme biosensors for the measurements of small input DNAs and RNAs. Based on the results from the experiments, it was observed that the sensitivity and detection limits of ribozyme-based sensors could be improved when deployed on DMF platforms.

4.4 Multiple ribozyme cleavage assays on a DMF chip

Additionally, a second DMF chip was designed to facilitate simultaneous experimentations via execution of multiple reactions on the same chip. Though the first chip had eight detection points, some of these fell along the paths of other detection points. Hence, the reagent droplets tend to leave traces and contaminate these detection points as they move across them, effectively limiting the number of experiments that can be done simultaneously to three.

The new chip consisted of 5 reservoirs to dispense reagents droplets, a 3 x 17 matrix of electrodes for moving, merging, and splitting the droplets, and 8 detection points for analyzing the assayed droplets. All the electrodes, detection points and reservoirs had the same dimensions, and had the same inter-electrode spacing and wiring widths as the first chip (Figure 18). The device dispensed droplets of size = $0.51 \pm 0.056 \mu\text{L}$ ($n = 10$) from $2.5 \mu\text{L}$ reagent droplets at the reservoirs. Experiments were carried out by dispensing ribozyme-containing droplets ($\sim 0.5 \mu\text{L}$) from the reservoirs and mixing and merging them with cleavage buffer droplets ($2 \mu\text{L}$) at the detection points, following the same procedure used on the first chip

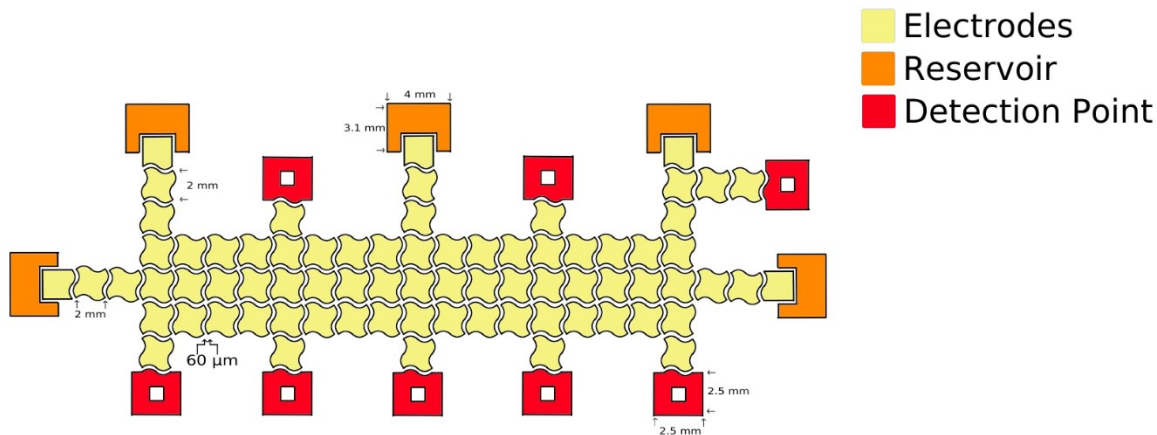


Figure 18: A schematic of a new DMF chip design to carry out eight simultaneous experiments.

The chip is comprised of eight detection points ($2.5 \times 2.5 \text{ mm}^2$), six reservoirs (each of $4 \times 3.1 \text{ mm}^2$) and a 3×17 matrix of electrodes (each of $2 \times 2 \text{ mm}^2$) for splitting, mixing and merging of droplets. In the design, the spacing between the electrode was $60 \mu\text{m}$.

The chip was successfully tested by carrying out two experiments. The first involved a ribozyme cleavage assay in triplicate (AS1, AS2 and AS3) with one positive control (PC, a strand displacement reaction) and one negative control (NC, a quenched probe). After performing the experiments on the chip, regular well-scans were taken every 4 min for 132 min (in appendix Figure 19), and the fluorescence intensities were plotted against time. In the second experiment, a ribozymatic experiment (AS) was performed on the new chip with one positive control (PC, strand displacement reaction) and five negative controls. The negative controls included a quenched probe in cleavage buffer (NC1), a buffer without MgCl_2 and input strand (NC2), buffer with MgCl_2 (NC3), buffer with input strand (NC4), and finally, buffer with a mutated input ssDNA and MgCl_2 (NC5). The assays followed the same steps as described in the section, DMF ribozyme cleavage assay in methodology, and regular fluorescence intensities of the assays were read every 9 min and plotted over time (Figure 20).

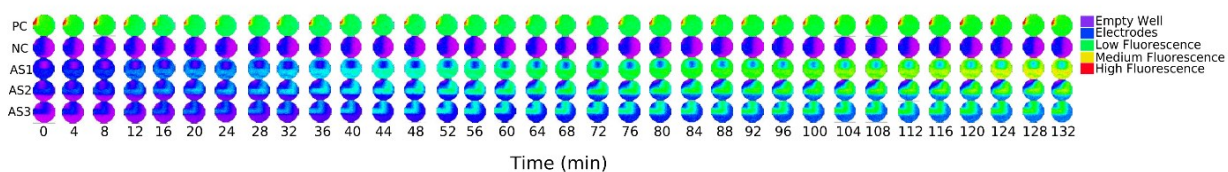


Figure 19: Ribozymatic assay in triplicates on a DMF chip.

A ribozymatic assay ($0.5 \mu\text{M}$ of ribozyme) is carried out on a chip in triplicates (AS1, AS2, AS3) with one positive (PC, a strand displacement reaction) and negative controls (NC, a quenched probe). After carrying out the experiments, the chip was scanned regularly in plate reading every 4 min for 132 min from the start of the experiment. The screenshots of well-scans corresponding to each assayed droplet on the DMF chip are recorded for all the readings. The positive control exhibited a high fluorescence throughout the experiment. At the same time, the negative control had a very low fluorescence intensity. However, all three assays displayed an increase in fluorescence after 20 min and reached a peak at the end of 132 min.

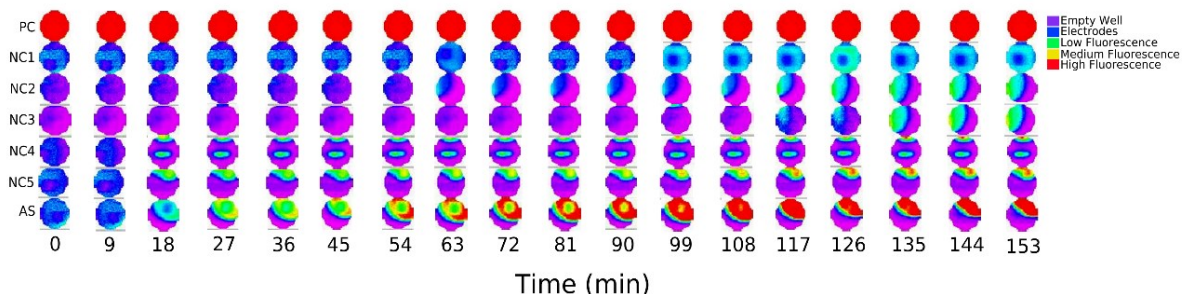


Figure 20: Multiple experiments performed simultaneously on a DMF chip.

The figure depicts well-scans of the DMF chip after carrying out a ribozyme cleavage reaction with one positive and five negative controls. The discs represent well-scans of the detection points taken every 9 min from the start of the experiment using a plate reader. The scans are arranged in rows and columns. Row corresponds to well-scans of a reaction throughout the experiment. Column depicts the scan of all the detection points at a specific time point. The reactions performed on the chip include ribozyme ($0.5 \mu\text{M}$) cleavage assay (AS), a strand displacement reaction as the positive control (PC), cleavage-buffer (NC1), cleavage-buffer with ribozyme (NC2), cleavage-buffer with ribozyme and input strand (NC3), cleavage-buffer with ribozyme and Mg^{+2} ions (NC4) and cleavage-buffer containing ribozyme, Mg^{+2} ions and mutated input strand (NC5). The positive control displays the highest level of fluorescence during the experimentation. All the negative controls except NC1 display a slight increase in fluorescence which could be due to the presence of inactive ribozyme in the solution, whereas NC1 exhibits a low level of fluorescence. However, the assay (AS) displays an increase in fluorescence intensities from 18 min and reached high values after 99 min, which indicated the cleavage of ribozyme as time progressed.

The results displayed the feasibility of carrying out multiple ribozymatic experiments, simultaneously, on one DMF chip. Such DMF platforms allow researchers to automate the initiation of ribozyme cleavage assays at the same time and monitor the progress of the reactions in real-time. Whereas in the well-plates, manual pipetting adds a delay between the initiations of these multiple reactions. Also, several identical DMF chips can be fabricated and operated in parallel, which further increases the number of experiments, thereby increasing the throughput of the experimental platform and reduces both labor costs and waiting time to final data collection.

Chapter 4: Summary and Conclusion

Ribozymes are used for many applications such as bio-sensing and as building blocks for genetic circuits. Thus, researchers have been keen on characterizing both the structure and function of ribozymes, in many cases, by analyzing their *cis*- and *trans*-cleavage kinetics, using a variety of techniques.

In this study, we designed a digital microfluidics (DMF) device, or chip, to perform multiple ribozymatic cleavage reactions while monitoring their progress in real-time. The chip used in-house software to manipulate droplets containing ribozyme, cleavage buffer and quenched probe, to ultimately initiate the cleavage reaction by mixing the droplets together. The single-stranded RNA output, of the ribozyme's self-cleavage reaction, displaces the quenching strand of the double-stranded DNA probe. This toehold mediated strand displacement reaction (TMSDR) allows us to indirectly monitor the progress of ribozyme self-cleavage, in real-time, using a fluorescence measuring plate reader.

The results from the study show that ribozyme cleavage experiments are reproducible on DMF chips. Moreover, these cleavage reactions proceeded at a greater rate (~2.5 times) than equivalent well-plate assays. In addition, we generated a standard curve relating the level of fluorescence (of probe) to the concentration of the single-stranded DNA input (of the self-cleaving ribozyme). The curve showed that the ribozyme on the DMF chip exhibited a greater level of sensitivity (~45% more than in well-plate) to DNA input and a lower limit of quantification ($\text{LoQ}_{\text{DMF}} = 0.025$) and limit of detection ($\text{LoD}_{\text{DMF}} = 1475$) than the same ribozyme in a well-plate ($\text{LoD}_{\text{Well-Plate}} = 1845$ and $\text{LoQ}_{\text{Well-Plate}} = 0.31$). The experiments with the DMF chips also generated reliable fluorescence readings with a signal to noise ratio equal to twice as much that in the well-plate. We also designed and tested a second DMF chip that allows for the execution of up to eight

parallel ribozyme cleavage reactions on the same chip (we carried out six experiments plus a positive and negative controls). Using multiple DMF chips is a swift and well-trodden path to scaling up the number of simultaneous experiments.

In brief, computer-controlled microfluidics devices offer ribozymatic researchers the ability to carry out multiple and different reactions using small volumes of reagents and involving minimal human intervention, while reading the output of these reactions as they progress, obviating (for many but not all cases) the need for post-reaction gels. This lowers experimental costs and time, while simultaneously increasing the quality of the harvested data, in terms of greater sensitivity and signal-to-noise ratio, as well as lower limit of quantification (LoQ) and limit of detection (LoD).

Chapter 5: Future Work

After demonstrating the successful application of DMF technology to the miniaturization and automation of ribozymatic experiments, the project could be expanded in the following two ways:

- First, by *optimizing DMF chip design*. The chip design can be further modified to manipulate smaller, possibly nL, droplets containing ribozyme and reagents, thereby minimizing reagents consumption during experiments. The chip can also be designed in such a way that a single contact point drives multiple electrodes. This facilitates the simultaneous actuation of multiple electrodes, leading to an increase in the number of concurrent experiments on one chip.
- Second, by *performing multi-step ribozymatic experiments*. The experiment only focused on a single-step ribozyme cleavage reaction. However, more complex and multi-step ribozymatic experiments, such as a biological relay or multi-input ribozyme-based gate reactions, can be performed on on DMF chips. After carrying out the first experiment, the same assayed droplet can be merged with a second reagent to initiate the second reaction without additional sampling. Similar experiments executed on the bench might require additional sampling and pipetting steps, which increases the likelihood of contamination and error.

References

- [1] “Nucleic Acid,” *Genome.gov*. <https://www.genome.gov/genetics-glossary/Nucleic-Acid> (accessed Nov. 01, 2020).
- [2] “Deoxyribonucleic Acid (DNA),” *Genome.gov*. <https://www.genome.gov/genetics-glossary/Deoxyribonucleic-Acid> (accessed Nov. 01, 2020).
- [3] “What is DNA?: MedlinePlus Genetics.” <https://medlineplus.gov/genetics/understanding/basics/dna/> (accessed Oct. 14, 2020).
- [4] “DNA and RNA structure: nucleic acids as genetic material,” *Medical Laboratory Observer*, Jan. 17, 2013. <https://www.mlo-online.com/home/article/13004885/dna-and-rna-structure-nucleic-acids-as-genetic-material> (accessed Nov. 01, 2020).
- [5] “WatsonCrick1953.pdf.” Accessed: Nov. 24, 2020. [Online]. Available: <http://dosequis.colorado.edu/Courses/MethodsLogic/papers/WatsonCrick1953.pdf>.
- [6] “Ribonucleic Acid (RNA),” *Genome.gov*. <https://www.genome.gov/genetics-glossary/RNA-Ribonucleic-Acid> (accessed Nov. 01, 2020).
- [7] D. L. Nelson, D. L. Nelson, A. L. Lehninger, and M. M. Cox, *Lehninger principles of biochemistry*. New York: W.H. Freeman, 2008.
- [8] K. Kruger, P. J. Grabowski, A. J. Zaug, J. Sands, D. E. Gottschling, and T. R. Cech, “Self-splicing RNA: autoexcision and autocyclization of the ribosomal RNA intervening sequence of Tetrahymena,” *Cell*, vol. 31, no. 1, pp. 147–157, Nov. 1982, doi: 10.1016/0092-8674(82)90414-7.
- [9] N. K. Tanner, “Ribozymes: the characteristics and properties of catalytic RNAs,” *FEMS Microbiol Rev*, vol. 23, no. 3, pp. 257–275, Jun. 1999, doi: 10.1111/j.1574-6976.1999.tb00399.x.

- [10] N. G. Walter and D. R. Engelke, “Ribozymes: Catalytic RNAs that cut things, make things, and do odd and useful jobs,” *Biologist (London)*, vol. 49, no. 5, pp. 199–203, Oct. 2002.
- [11] S. Ausländer, D. Fuchs, S. Hürlemann, D. Ausländer, and M. Fussenegger, “Engineering a ribozyme cleavage-induced split fluorescent aptamer complementation assay,” *Nucleic Acids Res*, vol. 44, no. 10, p. e94, Jun. 2016, doi: 10.1093/nar/gkw117.
- [12] C. Hammann, A. Luptak, J. Perreault, and M. de la Peña, “The ubiquitous hammerhead ribozyme,” *RNA*, vol. 18, no. 5, pp. 871–885, May 2012, doi: 10.1261/rna.031401.111.
- [13] D. M. J. Lilley and F. Eckstein, “Chapter 1: Ribozymes and RNA Catalysis: Introduction and Primer,” in *Ribozymes and RNA Catalysis*, 2007, pp. 1–10.
- [14] J. Wrzesinski, “Catalytic cleavage of cis- and trans-acting antigenomic delta ribozymes in the presence of various divalent metal ions,” *Nucleic Acids Research*, vol. 29, no. 21, pp. 4482–4492, Nov. 2001, doi: 10.1093/nar/29.21.4482.
- [15] J. Perreault *et al.*, “Identification of Hammerhead Ribozymes in All Domains of Life Reveals Novel Structural Variations,” *PLOS Computational Biology*, vol. 7, no. 5, p. e1002031, May 2011, doi: 10.1371/journal.pcbi.1002031.
- [16] G. A. Prody, J. T. Bakos, J. M. Buzayan, I. R. Schneider, and G. Bruening, “Autolytic processing of dimeric plant virus satellite RNA,” *Science*, vol. 231, no. 4745, pp. 1577–1580, Mar. 1986, doi: 10.1126/science.231.4745.1577.
- [17] A. C. Forster and R. H. Symons, “Self-cleavage of plus and minus RNAs of a virusoid and a structural model for the active sites,” *Cell*, vol. 49, no. 2, pp. 211–220, Apr. 1987, doi: 10.1016/0092-8674(87)90562-9.

- [18] J. M. Buzayan, W. L. Gerlach, and G. Bruening, “Non-enzymatic cleavage and ligation of RNAs complementary to a plant virus satellite RNA,” *Nature*, vol. 323, no. 6086, Art. no. 6086, Sep. 1986, doi: 10.1038/323349a0.
- [19] C. J. Hutchins, P. D. Rathjen, A. C. Forster, and R. H. Symons, “Self-cleavage of plus and minus RNA transcripts of avocado sunblotch viroid,” *Nucleic Acids Res*, vol. 14, no. 9, pp. 3627–3640, May 1986, doi: 10.1093/nar/14.9.3627.
- [20] J. M. Buzayan, A. Hampel, and G. Bruening, “Nucleotide sequence and newly formed phosphodiester bond of spontaneously ligated satellite tobacco ringspot virus RNA.,” *Nucleic Acids Res*, vol. 14, no. 24, pp. 9729–9743, Dec. 1986.
- [21] M. Anderson, E. P. Schultz, M. Martick, and W. G. Scott, “Active-site monovalent cations revealed in a 1.55-Å-resolution hammerhead ribozyme structure,” *J Mol Biol*, vol. 425, no. 20, pp. 3790–3798, Oct. 2013, doi: 10.1016/j.jmb.2013.05.017.
- [22] T.-S. Lee, C. S. López, G. M. Giambaşu, M. Martick, W. G. Scott, and D. York, “Role of Mg²⁺ in hammerhead ribozyme catalysis from molecular simulation.,” *Journal of the American Chemical Society*, 2008, doi: 10.1021/ja076529e.
- [23] D. E. Ruffner, G. D. Stormo, and O. C. Uhlenbeck, “Sequence Requirements of the Hammerhead RNA Self-Cleavage Reaction,” *BIOCHEM.J.*, vol. 29, no. 47, pp. 10695–10702, Nov. 1990, doi: 10.1021/bi00499a018.
- [24] R. Penchovsky, “Engineering Integrated Digital Circuits with Allosteric Ribozymes for Scaling up Molecular Computation and Diagnostics,” *ACS Synth. Biol.*, vol. 1, no. 10, pp. 471–482, Oct. 2012, doi: 10.1021/sb300053s.

- [25] R. Penchovsky, “Computational design and biosensor applications of small molecule-sensing allosteric ribozymes,” *Biomacromolecules*, vol. 14, no. 4, pp. 1240–1249, Apr. 2013, doi: 10.1021/bm400299a.
- [26] R. Penchovsky, “Computational design of allosteric ribozymes as molecular biosensors,” *Biotechnol. Adv.*, vol. 32, no. 5, pp. 1015–1027, Oct. 2014, doi: 10.1016/j.biotechadv.2014.05.005.
- [27] N. Kharma *et al.*, “Automated design of hammerhead ribozymes and validation by targeting the PABPN1 gene transcript,” *Nucleic Acids Res*, vol. 44, no. 4, pp. e39–e39, Feb. 2016, doi: 10.1093/nar/gkv1111.
- [28] R. Breaker, “Breaker, R.R. Engineered allosteric ribozymes as biosensor components. Curr. Opin. Biotechnol. 13, 31-39,” *Current opinion in biotechnology*, vol. 13, pp. 31–9, Mar. 2002, doi: 10.1016/S0958-1669(02)00281-1.
- [29] K. K. Singh, R. Parwaresch, and G. Krupp, “Rapid kinetic characterization of hammerhead ribozymes by real-time monitoring of fluorescence resonance energy transfer (FRET),” *RNA*, vol. 5, no. 10, pp. 1348–1356, Oct. 1999, doi: 10.1017/s1355838299991185.
- [30] T. K. Stage-Zimmermann and O. C. Uhlenbeck, “Hammerhead ribozyme kinetics,” *RNA*, vol. 4, no. 8, pp. 875–889, Aug. 1998.
- [31] S. Mercure, D. Lafontaine, S. Ananvoranich, and J.-P. Perreault, “Kinetic Analysis of δ Ribozyme Cleavage,” *Biochemistry*, vol. 37, no. 48, pp. 16975–16982, Dec. 1998, doi: 10.1021/bi9809775.
- [32] T. M. Picknett and S. Brenner, “Ribozymes,” in *Encyclopedia of Genetics*, S. Brenner and J. H. Miller, Eds. New York: Academic Press, 2001, p. 1730.

- [33] T. Tuschl, C. Gohlke, T. M. Jovin, E. Westhof, and F. Eckstein, “A three-dimensional model for the hammerhead ribozyme based on fluorescence measurements,” *Science*, vol. 266, no. 5186, pp. 785–789, Nov. 1994, doi: 10.1126/science.7973630.
- [34] T. A. Perkins, D. E. Wolf, and J. Goodchild, “Fluorescence resonance energy transfer analysis of ribozyme kinetics reveals the mode of action of a facilitator oligonucleotide,” *Biochemistry*, vol. 35, no. 50, pp. 16370–16377, Dec. 1996, doi: 10.1021/bi961234r.
- [35] N. G. Walter and J. M. Burke, “Real-time monitoring of hairpin ribozyme kinetics through base-specific quenching of fluorescein-labeled substrates,” *RNA (New York, N.Y.)*, vol. 3, no. 4, pp. 392–404, Apr. 1997.
- [36] B. G. Moreira, Y. You, M. A. Behlke, and R. Owczarzy, “Effects of fluorescent dyes, quenchers, and dangling ends on DNA duplex stability,” *Biochem. Biophys. Res. Commun.*, vol. 327, no. 2, pp. 473–484, Feb. 2005, doi: 10.1016/j.bbrc.2004.12.035.
- [37] N. Li, C. Yu, and F. Huang, “Novel cyanine-AMP conjugates for efficient 5' RNA fluorescent labeling by one-step transcription and replacement of [γ -³²P]ATP in RNA structural investigation,” *Nucleic Acids Res*, vol. 33, no. 4, p. e37, 2005, doi: 10.1093/nar/gni036.
- [38] M. Rb, E. La, M. Sr, L. Cj, and W. As, “Cyanine dye labeling reagents: sulfoindocyanine succinimidyl esters,” *Bioconjug Chem*, vol. 4, no. 2, pp. 105–111, Mar. 1993, doi: 10.1021/bc00020a001.
- [39] J. B. Kapadia, N. Kharma, A. N. Davis, N. Kamel, and J. Perreault, “Measurement of Kinetics of Hammerhead Ribozyme Cleavage Reactions using Toehold Mediated Strand Displacement,” *bioRxiv*, p. 2020.09.19.304931, Sep. 2020, doi: 10.1101/2020.09.19.304931.

- [40] T. L. Paxon *et al.*, “Continuous monitoring of enzyme reactions on a microchip: Application to catalytic RNA self-cleavage,” *Anal Chem*, vol. 76, no. 23, pp. 6921–6927, Jan. 2005, doi: 10.1021/ac0491758.
- [41] G. Linshiz *et al.*, “End-to-end automated microfluidic platform for synthetic biology: from design to functional analysis,” *Journal of Biological Engineering*, vol. 10, no. 1, p. 3, Feb. 2016, doi: 10.1186/s13036-016-0024-5.
- [42] T. A. Duncombe, A. M. Tentori, and A. E. Herr, “Microfluidics: reframing biological enquiry,” *Nat Rev Mol Cell Biol*, vol. 16, no. 9, pp. 554–567, Sep. 2015, doi: 10.1038/nrm4041.
- [43] A. Konda and S. A. Morin, “Flow-directed synthesis of spatially variant arrays of branched zinc oxide mesostructures,” *Nanoscale*, vol. 9, no. 24, pp. 8393–8400, 2017, doi: 10.1039/C7NR02655B.
- [44] “How to exploit the features of microfluidics technology,” *Lab Chip*, vol. 8, no. 1, pp. 20–22, 2008, doi: 10.1039/B717986N.
- [45] A. G. Hadd, D. E. Raymond, J. W. Halliwell, S. C. Jacobson, and J. M. Ramsey, “Microchip Device for Performing Enzyme Assays,” *Anal. Chem.*, vol. 69, no. 17, pp. 3407–3412, Sep. 1997, doi: 10.1021/ac970192p.
- [46] A. G. Hadd, S. C. Jacobson, and J. M. Ramsey, “Microfluidic Assays of Acetylcholinesterase Inhibitors,” *Anal. Chem.*, vol. 71, no. 22, pp. 5206–5212, Nov. 1999, doi: 10.1021/ac990591f.
- [47] M. A. Unger, H.-P. Chou, T. Thorsen, A. Scherer, and S. R. Quake, “Monolithic Microfabricated Valves and Pumps by Multilayer Soft Lithography,” *Science*, vol. 288, no. 5463, pp. 113–116, Apr. 2000, doi: 10.1126/science.288.5463.113.
- [48] “Tice et al. - 2013 - Normally-Closed Electrostatic Microvalve Fabricate.pdf.” .

- [49] C. Das and F. Payne, “Design and characterization of low power, low dead volume electrochemically-driven microvalve,” *Sensors and Actuators A: Physical*, vol. 241, pp. 104–112, Apr. 2016, doi: 10.1016/j.sna.2016.01.038.
- [50] P. J. Chang, F. W. Chang, M. C. Yuen, R. Otilar, and D. A. Horsley, “Force measurements of a magnetic micro actuator proposed for a microvalve array,” *J. Micromech. Microeng.*, vol. 24, no. 3, p. 034005, Mar. 2014, doi: 10.1088/0960-1317/24/3/034005.
- [51] J. Boutet *et al.*, “DNA repair enzyme analysis on EWOD fluidic microprocessor,” *undefined*, 2006. [/paper/DNA-repair-enzyme-analysis-on-EWOD-fluidic-Boutet-Castellan/3963ed5abf6ef3a60e7ecbc49530e25b4fafd231](#) (accessed Oct. 31, 2020).
- [52] J.-Y. Qian, C.-W. Hou, X.-J. Li, and Z.-J. Jin, “Actuation Mechanism of Microvalves: A Review,” *Micromachines*, vol. 11, no. 2, p. 172, Feb. 2020, doi: 10.3390/mi11020172.
- [53] B. J. Burke and F. E. Regnier, “Stopped-Flow Enzyme Assays on a Chip Using a Microfabricated Mixer,” *Anal. Chem.*, vol. 75, no. 8, pp. 1786–1791, Apr. 2003, doi: 10.1021/ac026173j.
- [54] C. L. Hansen, M. O. A. Sommer, S. R. Quake, and R. H. Austin, “Systematic Investigation of Protein Phase Behavior with a Microfluidic Formulator,” *Proceedings of the National Academy of Sciences of the United States of America*, vol. 101, no. 40, pp. 14431–14436, 2004.
- [55] H. Song, J. D. Tice, and R. F. Ismagilov, “A microfluidic system for controlling reaction networks in time,” *Angew. Chem. Int. Ed. Engl.*, vol. 42, no. 7, pp. 768–772, Feb. 2003, doi: 10.1002/anie.200390203.
- [56] P. Garstecki, M. J. Fuerstman, H. A. Stone, and G. M. Whitesides, “Formation of droplets and bubbles in a microfluidic T-junction—scaling and mechanism of break-up,” *Lab Chip*, vol. 6, no. 3, p. 437, 2006, doi: 10.1039/b510841a.

- [57] C. Baroud, F. Gallaire, and R. Dangla, “Dynamics of microfluidic droplets,” *Lab on a chip*, vol. 10, pp. 2032–45, Aug. 2010, doi: 10.1039/c001191f.
- [58] N. Bremond, A. R. Thiam, and J. Bibette, “Decompressing Emulsion Droplets Favors Coalescence,” *Phys. Rev. Lett.*, vol. 100, no. 2, p. 024501, Jan. 2008, doi: 10.1103/PhysRevLett.100.024501.
- [59] T. H. Ting, Y. F. Yap, N.-T. Nguyen, T. N. Wong, J. C. K. Chai, and L. Yobas, “Thermally mediated breakup of drops in microchannels,” *Appl. Phys. Lett.*, vol. 89, no. 23, p. 234101, Dec. 2006, doi: 10.1063/1.2400200.
- [60] H. Song, M. R. Bringer, J. D. Tice, C. J. Gerdtts, and R. F. Ismagilov, “Experimental test of scaling of mixing by chaotic advection in droplets moving through microfluidic channels,” *Appl Phys Lett*, vol. 83, no. 12, pp. 4664–4666, Dec. 2003, doi: 10.1063/1.1630378.
- [61] S.-Y. Teh, R. Lin, L.-H. Hung, and A. P. Lee, “Droplet microfluidics,” *Lab Chip*, vol. 8, no. 2, pp. 198–220, Jan. 2008, doi: 10.1039/B715524G.
- [62] M. Abdelgawad and A. R. Wheeler, “The Digital Revolution: A New Paradigm for Microfluidics,” *Adv. Mater.*, vol. 21, no. 8, pp. 920–925, Feb. 2009, doi: 10.1002/adma.200802244.
- [63] E. M. Miller and A. R. Wheeler, “Digital bioanalysis,” *Anal Bioanal Chem*, vol. 393, no. 2, pp. 419–426, Jan. 2009, doi: 10.1007/s00216-008-2397-x.
- [64] C. Quilliet and B. Berge, “Electrowetting: a recent outbreak,” *Current Opinion in Colloid & Interface Science*, vol. 6, no. 1, pp. 34–39, Feb. 2001, doi: 10.1016/S1359-0294(00)00085-6.
- [65] K. Choi, A. H. C. Ng, R. Fobel, and A. R. Wheeler, “Digital Microfluidics,” *Annual Review of Analytical Chemistry*, vol. 5, no. 1, pp. 413–440, 2012, doi: 10.1146/annurev-anchem-062011-143028.

- [66] M. Washizu, “Electrostatic actuation of liquid droplets for micro-reactor applications,” 1997, doi: 10.1109/28.703965.
- [67] M. G. Pollack, R. B. Fair, and A. D. Shenderov, “Electrowetting-based actuation of liquid droplets for microfluidic applications,” *Appl. Phys. Lett.*, vol. 77, no. 11, pp. 1725–1726, Sep. 2000, doi: 10.1063/1.1308534.
- [68] M. Pollack, R. Fair, and A. Shenderov, “Pollack, M. G., Fair, R. B. & Shenderov, A. D. Electrowetting-based actuation of liquid droplets for microfluidic applications. *Appl. Phys. Lett.* 77, 1725–1726,” *Applied Physics Letters*, vol. 77, pp. 1725–1726, Sep. 2000, doi: 10.1063/1.1308534.
- [69] Sung Kwon Cho, Hyejin Moon, and Chang-Jin Kim, “Creating, transporting, cutting, and merging liquid droplets by electrowetting-based actuation for digital microfluidic circuits,” *J. Microelectromech. Syst.*, vol. 12, no. 1, pp. 70–80, Feb. 2003, doi: 10.1109/JMEMS.2002.807467.
- [70] E. M. Miller and A. R. Wheeler, “A Digital Microfluidic Approach to Homogeneous Enzyme Assays,” *Anal. Chem.*, vol. 80, no. 5, pp. 1614–1619, Mar. 2008, doi: 10.1021/ac702269d.
- [71] L. M. Y. Leclerc, G. Soffer, D. H. Kwan, and S. C. C. Shih, “A fucosyltransferase inhibition assay using image-analysis and digital microfluidics,” *Biomicrofluidics*, vol. 13, no. 3, p. 034106, May 2019, doi: 10.1063/1.5088517.
- [72] P. Q. N. Vo, M. C. Husser, F. Ahmadi, H. Sinha, and S. C. C. Shih, “Image-based feedback and analysis system for digital microfluidics,” *Lab Chip*, vol. 17, no. 20, pp. 3437–3446, Oct. 2017, doi: 10.1039/C7LC00826K.
- [73] D. Hess, T. Yang, and S. Stavrakis, “Droplet-based optofluidic systems for measuring enzyme kinetics,” *Anal Bioanal Chem*, vol. 412, no. 14, pp. 3265–3283, May 2020, doi: 10.1007/s00216-019-02294-z.

- [74] C. B. Cohen, E. Chin-Dixon, S. Jeong, and T. T. Nikiforov, “A Microchip-Based Enzyme Assay for Protein Kinase A,” *Analytical Biochemistry*, vol. 273, no. 1, pp. 89–97, Aug. 1999, doi: 10.1006/abio.1999.4204.
- [75] J. J. Agresti *et al.*, “Ultrahigh-throughput screening in drop-based microfluidics for directed evolution,” *Proc. Natl. Acad. Sci. U.S.A.*, vol. 107, no. 9, pp. 4004–4009, Mar. 2010, doi: 10.1073/pnas.0910781107.
- [76] S. C. C. Shih *et al.*, “A droplet-to-digital (D2D) microfluidic device for single cell assays,” *Lab Chip*, vol. 15, no. 1, pp. 225–236, Jan. 2015, doi: 10.1039/c4lc00794h.
- [77] M. Abdelgawad and A. R. Wheeler, “Low-cost, rapid-prototyping of digital microfluidics devices,” *Microfluid Nanofluid*, vol. 4, no. 4, pp. 349–355, Apr. 2008, doi: 10.1007/s10404-007-0190-3.
- [78] M. Abdelgawad and A. R. Wheeler, “Rapid Prototyping in Copper Substrates for Digital Microfluidics,” *Advanced Materials*, vol. 19, no. 1, pp. 133–137, 2007, doi: 10.1002/adma.200601818.
- [79] M. Ryckelynck *et al.*, “Using droplet-based microfluidics to improve the catalytic properties of RNA under multiple-turnover conditions,” *RNA*, vol. 21, no. 3, pp. 458–469, Mar. 2015, doi: 10.1261/rna.048033.114.
- [80] B. J *et al.*, “DNA repair enzyme analysis on EWOD fluidic microprocessor,” *TechConnect Briefs*, vol. 2, no. 2006, pp. 554–557, May 2006.
- [81] S. Tian and R. Das, “Primerize-2D: Automated primer design for RNA multidimensional chemical mapping,” *Bioinformatics (Oxford, England)*, vol. 33, Jan. 2017, doi: 10.1093/bioinformatics/btw814.

- [82] K. Samlali, F. Ahmadi, A. B. V. Quach, G. Soffer, and S. C. C. Shih, “One Cell, One Drop, One Click: Hybrid Microfluidics for Mammalian Single Cell Isolation,” *Small*, vol. n/a, no. n/a, p. 2002400, doi: 10.1002/sml.202002400.
- [83] T. Taniguchi, T. Torii, and T. Higuchi, “Chemical reactions in microdroplets by electrostatic manipulation of droplets in liquid media,” *Lab on a Chip*, vol. 2, no. 1, pp. 19–23, 2002, doi: 10.1039/B108739H.
- [84] M. Skilandat and R. K. O. Sigel, “Ribozymes,” in *Brenner’s Encyclopedia of Genetics (Second Edition)*, S. Maloy and K. Hughes, Eds. San Diego: Academic Press, 2013, pp. 254–258.
- [85] A. Jenne *et al.*, “Rapid identification and characterization of hammerhead-ribozyme inhibitors using fluorescence-based technology,” *Nature Biotechnology*, vol. 19, no. 1, Art. no. 1, Jan. 2001, doi: 10.1038/83513.
- [86] J. Berthier and C. Peponnet, “A model for the determination of the dimensions of dents for jagged electrodes in electrowetting on dielectric microsystems,” *Biomicrofluidics*, vol. 1, no. 1, p. 014104, Dec. 2006, doi: 10.1063/1.2409626.
- [87] F. Ahmadi, K. Samlali, P. Q. N. Vo, and S. C. C. Shih, “An integrated droplet-digital microfluidic system for on-demand droplet creation, mixing, incubation, and sorting,” *Lab Chip*, vol. 19, no. 3, pp. 524–535, Jan. 2019, doi: 10.1039/C8LC01170B.
- [88] M. Abdelgawad, P. Park, and A. R. Wheeler, “Optimization of device geometry in single-plate digital microfluidics,” *Journal of Applied Physics*, vol. 105, no. 9, p. 094506, May 2009, doi: 10.1063/1.3117216.
- [89] N. Rajabi and A. Dolatabadi, “A novel electrode shape for electrowetting-based microfluidics,” *Colloids and Surfaces A: Physicochemical and Engineering Aspects*, vol. 365, no. 1, pp. 230–236, Aug. 2010, doi: 10.1016/j.colsurfa.2010.01.039.

- [90] V. Srinivasan, V. K. Pamula, and R. B. Fair, “Droplet-based microfluidic lab-on-a-chip for glucose detection,” *Analytica Chimica Acta*, vol. 507, no. 1, pp. 145–150, Apr. 2004, doi: 10.1016/j.aca.2003.12.030.
- [91] M. Pollack, A. Shenderov, and R. B. Fair, “Electrowetting-based actuation of droplets for integrated microfluidics,” *Lab on a chip*, 2002, doi: 10.1039/B110474H.
- [92] S. Mercure, D. Lafontaine, S. Ananvoranich, and J.-P. Perreault, “Kinetic Analysis of δ Ribozyme Cleavage,” *Biochemistry*, vol. 37, no. 48, pp. 16975–16982, Dec. 1998, doi: 10.1021/bi9809775.
- [93] R. Kwapiszewski, J. Szczudlowska, K. Kwapiszewska, A. Dybko, and Z. Brzozka, “Effect of downscaling on the linearity range of a calibration curve in spectrofluorimetry,” *Anal Bioanal Chem*, vol. 406, no. 18, pp. 4551–4556, 2014, doi: 10.1007/s00216-014-7844-2.
- [94] M. Tabaka, T. Kalwarczyk, J. Szymanski, S. Hou, and R. Holyst, “The effect of macromolecular crowding on mobility of biomolecules, association kinetics, and gene expression in living cells,” *Front. Phys.*, vol. 2, 2014, doi: 10.3389/fphy.2014.00054.
- [95] P. T. Sekella, D. Rueda, and N. G. Walter, “A biosensor for theophylline based on fluorescence detection of ligand-induced hammerhead ribozyme cleavage,” *RNA*, vol. 8, no. 10, pp. 1242–1252, Oct. 2002.
- [96] G. Gauglitz, “Analytical evaluation of sensor measurements,” *Anal Bioanal Chem*, vol. 410, no. 1, pp. 5–13, Jan. 2018, doi: 10.1007/s00216-017-0624-z.
- [97] Á. Lavín *et al.*, “On the Determination of Uncertainty and Limit of Detection in Label-Free Biosensors,” *Sensors (Basel)*, vol. 18, no. 7, Jun. 2018, doi: 10.3390/s18072038.
- [98] “Limit of Blank (LOB), Limit of Detection (LOD), and Limit of Quantification (LOQ),” *Organic and Medicinal Chemistry International Journal*, p. 5.

[99] M. Thompson, S. Ellison, and R. Wood, “Harmonized guidelines for single-laboratory validation of methods of analysis (IUPAC Technical Report),” 2002, doi: 10.1351/pac200274050835.

[100] X. Li, C. Zhao, and X. Liu, “A paper-based microfluidic biosensor integrating zinc oxide nanowires for electrochemical glucose detection,” *Microsystems & Nanoengineering*, vol. 1, no. 1, Art. no. 1, Aug. 2015, doi: 10.1038/micronano.2015.14.

Appendices

Appendix 1: User Manual



RIBOZYME ASSAY ON DMF CHIP USER MANUAL

Alen Nellikulam Davis
alendvs@yahoo.co.in

Contents

Preparation	63
List of all materials.....	63
Safety protocols.....	64
Overview	65
Probe Preparation.....	65
Required Materials	65
Procedure.....	66
Chip Fabrication	67
Required Materials	67
Procedure.....	68
Experiments on the Bench.....	70
Required Materials	70
Procedure.....	71
Experiments on DMF Chip	71
Required Materials	71
Procedure.....	72
Reading fluorescence	81
Required Materials	81
Procedure.....	81

Preparation

List of all materials

Item	Stock Quantity/Concentration
Deionized (DI) water	
Iso Propyl Alcohol (IPA)	
RNase away	
Pipette	
Pipette tips	
PCR tubes	100 μ L
Corning [®] 384 Flat-black, clear bottom well plate	
Tris HCl pH 7.5	106 μ M
KCl	106 μ M
NaCl	106 μ M
MgCl ₂	106 μ M
Input single stranded DNA (ssDNA)	100 μ M
Cy-5 Fluorophore	100 μ M
Black Hole Quencher	100 μ M
Tetronics	0.60%
Nuclease-Free Water	
KIM wipes	
microfuge tubes	1.5 mL
Thermocycler	
Plate reader	
Aluminum Foil	
Lab Coat	
Hair Net	
Disposable shoe covers	
Gloves	
Chip Masks	
Photoresist-coated substrates	
4"x4" glass slides	

Acetone	
Methanol	
Spin Coater	
S1811 Photoresist	
MF321 developer	
Chromium Etchant (CR-4)	
AZ300T stripper	
2-propanol	
A-174 (3-(Trimethoxysilyl)propyl methacrylate)	
Parylene	
Teflon-AF (FC40) or Cytonix	
Pyrex dishes	
Tweezers	
Hot plate	
Ribozyme	
Cleavage buffer with quenched probe	
Output Strand	
Pipettes	
Parafilm	
Ice	
Automation System	
Digital Microfluidics (DMF) chips	
Top Plate coated with indium tin oxide (ITO)	
Teflon-AF	
Multimeter	

Safety protocols

- Wear lab coats when inside a lab.
- Wear gloves during experimentation.
- Use RNase away as much as possible when working with ribozyme.
- After usage, store all the reagents at **-20°C**.

Overview

This manual describes the protocol for carrying out a ribozyme cleavage experiment on a well-plate and DMF chip. The experiment uses a Toehold mediated strand displacement reaction to monitor the progress of the ribozyme's cleavage. The experiment begins with the preparation of a double stranded DNA probe, which is used as a target for the active ribozyme's cleaved-off strand. The experiments are performed both on the well-plate and DMF chip, after which, both the platforms can be scanned using a fluorescent plate reader.

Probe Preparation

Required Materials

Item	Stock Quantity/Concentration
DI water	
Iso Propyl Alcohol (IPA)	
RNAse away	
Pipette	
Pipette tips	
PCR tubes	100 μ L
Black sided flat bottom 384 well-plate	
Tris HCl pH 7.5	10 ⁶ μ M
KCl	10 ⁶ μ M
NaCl	10 ⁶ μ M
MgCl ₂	10 ⁶ μ M
Input single stranded DNA (ssDNA)	100 μ M
Cy-5 Fluorophore	100 μ M
Black Hole Quencher-3	100 μ M
Tetronics	0.6%

Nuclease-Free Water	
KIM wipes	
Microfuge tubes	1.5 mL
Thermocycler	
Fluorescent Plate reader	
Aluminum Foil	

Procedure

1. Bench and Tools Cleaning
 - a. Always wear lab coat and gloves when working in the lab
 - b. Use RNase away, and DI water on the hands as needed to keep them clean.
 - c. Use/Spray RNase away on the bench and wipe using KIM wipes.
 - d. Sprinkle iso-propyl alcohol (IPA) on the bench and clean using KIM wipes.
 - e. Finally clean the bench with water and wipe using KIM wipes.
 - f. Clean the Tools (mainly the pipettes) by following the steps **c-e**.
2. Work under aseptic conditions if possible (Optional).
3. Protocol to prepare 200 uL of Quenched Probe
 - a. Grab 1.5 mL microfuge tube.
 - b. To the tube add **26.4 μL** of **NaCl ($10^6 \mu\text{M}$)**.
 - c. Add and mix **13.2 μL** of **Tris ($10^6 \mu\text{M}$)**.
 - d. Add and mix **6.6 μL** of **KCl ($10^6 \mu\text{M}$)**.
 - e. Add and mix **0.264 μL** of **MgCl₂($10^6 \mu\text{M}$)**
 - f. Add and mix **2.64 μL** of **Input ssDNA ($100 \mu\text{M}$)**.
 - g. Add and mix **1.32 μL** of **Cy-5 Fluorophore ($100 \mu\text{M}$)**.
 - h. Add and mix **136.651 μL** of **Nuclease-free Water**.
 - i. From the take-out a sample of **9.92 μL** and add it into a well in the well-plate (corning flat-black clear bottom 384)
 - j. To the sampled mixture in the well-plate, add **0.08 μL** of **Nuclease-free Water**.
 - k. Cover the well-plate with its lid.
 - l. Place the well-plate in a fluorescent plate reader.
 - m. Set the temperature to **37°C**.
 - n. Set the excitation and emission wavelengths to be $\lambda_{\text{ex}} = 647 \text{ nm}$, $\lambda_{\text{em}} = 665 \text{ nm}$.
 - o. Take the fluorescence reading of the sample.
 - p. To the mixture at step **h**, add and mix **1.42 μL** of **Quencher ($100 \mu\text{M}$)**.
 - q. Split new mixture to mini batches of **90 μL** in PCR tubes.

- r. Place the PCR tubes in a thermocycler and perform the following:
 - i. **3 min** denaturation at **95°C**
 - ii. **15 min** annealing at **50°C**, and
 - iii. **15 min** incubation at **37°C**.
- s. Add and mix **10 μL** of **Tetronics (0.6%)** to all resultant batches.
- t. Take out samples (**10 μL**) from all the batches to a well-plate.
- u. Read the fluorescence of the new samples by following the steps “**k-o**”.
- v. Ensure that the readings at step “**u**” are lower than readings from step “**o**”. Else repeat protocol again.
- w. Carefully wrap the PCR tubes with the prepared probe in step ‘**s**’ with Aluminum foil.
- x. Finally, store the tubes in a freezer at **-20°C**.

***Note:** Please note the volumes of the reagents were determined with the assumption that the experiments on bench were performed by mixing the 8 μL of the above probe mixture and 2 μL of ribozyme. The same experiment on the DMF chip would be performed by mixing 2 μL of probe with 0.5 μL of ribozyme. Final assay contains NaCl (100 mM), Tris (50 mM), KCl (25 mM), MgCl₂ (10 mM), input ssDNA (1 μM), quenched probe (0.5 μM), and ribozyme (0.5 μM).*

Chip Fabrication

Required Materials

Item	Stock Quantity/Concentration
Lab Coat	
Hair Net	
Disposable shoe covers	
Gloves	
Chip Masks	
Photoresist-coated substrates	
4"x4" glass slides	
Acetone	
Methanol	

DI water	
Spin Coater	
S1811 Photoresist	
MF321 developer	
Chromium Etchant	
AZ300T stripper	
2-propanol	
A-174 (3-(Trimethoxysilyl)propyl methacrylate)	
Parylene	
Teflon	
Pyrex dishes	3-4
Tweezers	
Hot plate	

Procedure

1. Safety

- a. As soon as you enter the cleanroom, put on following personal protective equipment:
 - i. Lab coat
 - ii. Hair net
 - iii. Disposable shoe covers
 - iv. Gloves

2. Exposure (patterning the photoresist with your design)

- a. When you get in the UV-negative cleanroom, turn on the power of the UV lamp.
- b. After a few minutes, turn the lamp on by pressing on the switch for a few seconds. Let the lamp heat up for 10 minutes.
- c. Turn on the vacuum (power strip)
- d. In the meantime, prepare the masks by cutting them to the right size and sticking them in the middle of the glass 4"x4" slides using the circular adhesives in the **proper** orientation (Make sure not to tape over any part of your design). The

mask should be taped under the glass – in the exposure, the plastic mask should be in contact with the substrate to prevent UV diffraction.

- e. Next, cut your photoresist-coated substrates to the desired size.

Note: if you have a scratch on the photoresist:

- Wash with acetone (removes photoresist)
- Rinse with methanol
- Rinse with water
- Spin coat S1811 photoresist
- 10 sec 500 RPM Accel = 100 RPM/s
- 60 sec 3000 RPM Accel = 500 RPM/s
- Bake at 105° for 2 min to remove solvent

- f. Place the glass mask on the mask holder (plastic mask on the bottom side) and make sure that it is vacuumed properly.
- g. Place substrate and align manually with the mask. Then fine tune with the knob.
- h. Expose for 10 sec.

3. Development (removes the photoresist at exposed regions – transparent regions of mask)

- a. Move under the hood in the same room.
- b. Immerse the slides in the MF321 developer in Pyrex dish and shake around for 2 min.
- c. Rinse with DI and air dry.
- d. Bake at 115° for 1min each.
- e. Discard waste in MF321 waste container (use funnel).

4. Etching (corrodes the exposed metal layer – no longer has photoresist on it after development)

- a. Move to the wet bench in the annex room for etching. Turn on the vent.
Note: Respect the PPE (wear a face shield, long rubber gloves and apron).
- b. Place substrates in a Pyrex dish and immerse with Chromium Etchant solution.
Note Work slowly to minimize spills and splashes. Manipulate substrates with care using tweezers.
- c. Wait until all the substrates become transparent except the pattern (3-5min), shake around.
- d. Rinse substrates well with DI.
- e. Discard waste into the Chromium-Etchant (Cr-4) waste container.

5. Stripping (removes all the remaining photoresist from non-exposed regions)

- a. Move to the small wet bench room with the windows for stripping.
Note: Work under the hood of a wet bench – the vapors of the stripper are toxic.
- b. Immerse substrates in AZ 300T Stripper solution. Shake around for a few minutes.
- c. Rinse well with DI.
- d. Air dry the substrates.
- e. Discard waste in AZ400T waste container.

6. Silanization (coats the surface with alkoxy silane molecules to increase Parylene adherence)
 - a. Prepare Silane solution
 - i. *2-propanol, DI water, and A-174 (3-(Trimethoxysilyl) propyl methacrylate) 50:50:1 v/v/v*
 - b. Immerse substrates in silane solution. Leave for 15 min.
 - c. Rinse with DI and air dry.
 - d. Discard silane solution in silane waste container.

7. Parylene coating (coats the slides with a layer of dielectric material)
 - a. Move to the room for Parylene Coating by chemical vapor deposition.
 - b. Put yellow tape on the contact pads prior to coating.
 - c. Place substrates in the chamber with the patterned side up.
 - d. Add 8g of Parylene C to the furnace for an intended thickness of approximately 3 μ m.

8. Teflon coating (coats the slides with a hydrophobic layer)
 - a. Spin coat substrates with 1% Teflon-AF in FC40. (or use Cytonix solution)
 - i. 30 sec 500 RPM Accel = 100 RPM/s
 - ii. 60 sec 3000 RPM Accel = 500 RPM/s
 - b. Bake for 10min at 160°C to remove the solvent.

Experiments on the Bench

Required Materials

Item	Stock Quantity/Concentration
Ribozyme	
Cleavage buffer with quenched probe	
Black sided flat bottom 384 well-plate	
Output Strand	
Pipettes	
Pipette tips	
Parafilm	
Ice	

Procedure

1. Bench and tools cleaning:
 - a. When inside the lab, wear lab coats and gloves before starting the experiments.
 - b. Use RNase away, and DI water on the hands as needed to prevent contamination.
 - c. Use/Spray RNase away on the bench and wipe using KIM wipes.
 - d. Sprinkle IPA on the bench and clean using KIM wipes.
 - e. Finally clean the bench with water and wipe it using KIM wipes.
 - f. Clean the Tools (mainly the pipettes) by following the steps **c-e**.
 - g. Try to work under aseptic condition (optional).

2. Experimentation
 - a. In a container add some ice.
 - b. Grab aliquots of ribozyme, output strand and cleavage buffer with quenched probe from the refrigerator.
 - c. Place the ribozyme and buffer containing tubes in the container with ice.
 - d. Using a pipette, add **8 μL** to three well (W1-W3) in a 384 well-plate.
 - e. Add **2 μL** of DI water to W1 and mix carefully. Assay in this well will be used as the negative control (Quenched probe).
 - f. Add **2 μL** of output strand to W2 and mix carefully. Assay in this well will be used as the positive control (Unquenched probe).
 - g. Add **2 μL** of ribozyme to W3 and mix carefully. This serves as the ribozyme cleavage assay.
 - h. Perform steps **d-g** in different wells to have multiple repeats of the experiments.
 - i. Additionally add **30 μL** to five wells around the assays in the well-plate to maintain the humidity within the plate.
 - j. Cover the plate with its lid and seal the sides using parafilm.

Experiments on DMF Chip

Required Materials

Item	Stock Quantity/Concentration
Ribozyme	
Cleavage buffer with quenched probe	
Black sided flat bottom 384 well-plate	

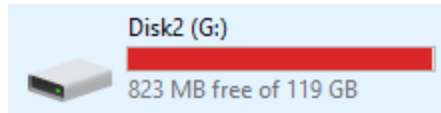
Output Strand	
Pipettes	
Pipette tips	
Parafilm	
Automation System	
Plate reader	
DMF chips	
Top Plate (ITO)	
Teflon-AF	
Spin Coater	
Multimeter	
RNAse away	
DI water	
IPA	
Kim Wipes	

Procedure

1. Bench and tools cleaning:
 - a. When inside the lab, wear lab coats and gloves before starting the experiments.
 - b. Use RNAse away, and DI water on the hands as needed to prevent contamination.
 - c. Use/Spray RNAse away on the bench and wipe using KIM wipes.
 - d. Sprinkle IPA on the bench and clean using KIM wipes.
 - e. Finally clean the bench with water and wipe using KIM wipes.
 - f. Clean the Tools (mainly the pipettes, chips and top plate) by following the steps **c-e**.

2. Preparing top plate:
 - a. Grab a **glass plate coated with ITO** (Indium Tin Oxide)
 - b. Cut the Plate into two halves.
 - c. Make note of the **ITO-coated** side using a **multimeter**.

- i. Turn the dial on the multimeter and keep it pointed to resistance (Ω) measurements.
 - ii. Place both the ends of the multimeter on the desired side of the glass slide.
 - iii. If the multimeter shows some reading, it is an indication that the current side of the glass slide is coated with ITO.
 - iv. Perform steps **i-iii** for all the plates.
 - d. Coat the ITO-coated side of the top plate with a hydrophobic layer.
 - i. Spin coat substrates with 1% Teflon-AF in FC40. (or use Cytonix solution)
 - 30 sec 500 RPM Accel = 100 RPM/s
 - 60 sec 3000 RPM Accel = 500 RPM/s
 - ii. Bake for 10min at 160°C to remove the solvent.
3. Setting up the automation system:
- a. Connect the rainbow cables from the stack of switches to the pogo pin board by ensuring that the labels on the either side matches
Note: If not please get help from Shih Lab.
 - b. Make sure that the following connections to the control board are correct:
 - i. SCL to arduino's SCL
 - ii. SDA to arduino's SDA
 - iii. Connect 5V to (+) of the power supply
 - iv. Connect GND to (-) of the power supply
 - v. Connect AMP to (red) Amplifier probe
 - vi. Connect H_GND to (black) Amplifier probe
 - vii. Arduino GND to (-) of power supply
Note: All these connections are clearly labelled. Please reach out to Shih Lab if a cable is missing or in case of any additional queries.
 - c. Setting up the function generator:
 - i. Switch ON the function generator.
 - ii. Select sine wave.
 - iii. Set the frequency to 15 kHz.
 - iv. Set the amplitude to 2.2 Vpp
 - d. Setting up the power supply:
 - i. Switch on the power supply.
 - ii. Set the output to ON.
 - iii. Set to 25 range by clicking on the 25+ button.
 - iv. Apply 5V
 - e. Connect the H_GND cable and connect to the top plate (ITO).
 - f. Load the DMF chip onto the pogo pin board by carefully aligning the contact point to the pogo pins.
 - g. Tighten the screws on the board to ensure that the pins touch the contact points
4. Setting up the software:
- a. Open the folder "**Alen**" from G-drive.



Alen

- b. Open the folder **Design1** or **Design2** depending on the chip that you used to carry out the experiment.

Design1	24-Aug-19 7:13 PM	File folder
Design2	26-Aug-19 6:11 PM	File folder

- c. Open the folder **Codes**.

Codes

- d. Open the file **ArduBridgeaAlen.py** in the editor.

ArduBridgeaAlen.py	16-Jan-19 9:37 AM	Python File	5 KB
ArduBridgeaAlen.pyc	23-Oct-19 8:22 PM	Compiled Python ...	4 KB
LLGUI_KS.py	07-Aug-18 3:09 PM	Python File	10 KB
LLGUI_KS.pyc	30-Mar-19 5:28 PM	Compiled Python ...	9 KB
pins (7).ods	14-Oct-19 7:25 PM	OpenDocument S...	6 KB
protocol_Alen.py	14-Oct-19 4:47 PM	Python File	32 KB
protocol_Alen.pyc	14-Oct-19 4:49 PM	Compiled Python ...	14 KB
UdpTo_wxChipViewer.bat	22-Feb-19 2:39 PM	Windows Batch File	1 KB
vine_grid_LL.cfg	20-Mar-18 1:05 PM	CFG File	2 KB
Vine2ProtocolTopSteps.py	23-Jul-18 5:19 PM	Python File	38 KB
Vine2ProtocolTopSteps.pyc	22-Feb-19 2:30 PM	Compiled Python ...	19 KB

```
ArduBridgeaAlen.py - G:\Alen\Design1\Codes\ArduBridgeaAlen.py (2.7.14)
File Edit Format Run Options Window Help
#!/usr/bin/env python
"""
Script to build an ArduBridge environment
To customize the environment to your needs. You will need to change
he parameters in the "PARAMETER BLOCK" in the __main__ section

By: Guy Soffer
Date: 11/June/2018

Edit by Kenza
Date: 07/08/18

"""
##### RUN CHIPVIEWER AND LLGUI AFTER RUNNING THIS FILE #####
#Basic modules to load
import time
from GSOE_ArduBridge import udpControl
from GSOE_ArduBridge import ArduBridge
from GSOE_ArduBridge import ElectrodeGpioStack
from GSOE_ArduBridge import threadPID
from GSOE_ArduBridge import UDP_Send

def extEval(s):
    s=str(s)
    eval(s)

def close():
    if udpConsol != False:
        udpConsol.active = False
    setup.stop()
    ardu.OpenClosePort(0)
    print 'Bye Bye...'

def tempTC1047(pin=0, vcc=5.0):
    b = ardu.an.analogRead(pin)
    v = b*vcc/1024.0
    T = 100*(v -0.5)

if __name__ == "__main__":
    #\\\\\\ CHANGE THESE PARAMETERS \\\\/\

Ln: 1 Col: 0
```

e. Press F5. This opens a terminal with messages.

Note: In case of error, type close() in the terminal and press ENTER. Then open the task managers and close all currently running python processes. Restart the terminal by pressing F5 as in steps “c-d”


```

protocol_Alen.py - G:\Alen\Design1\Codes\protocol_Alen.py (2.7.14)
File Edit Format Run Options Window Help

"""
If ERRs at start,
ExtGpio.init()
"""

try:
    from GSOF_ArduBridge import threadElectrodeSeq
except ImportError:
    threadElectrodeSeq = False
    class dummyThread():
        def __init__(self, nameID):
            self.name = nameID

from GSOF_ArduBridge import threadBasic as bt
import time

class Protocol(bt.BasicThread):
    """
    Period is the step period-time. If T == 0, The process will run only once.
    """
    def __init__(self, setup=False, nameID='SPE1', Period=1, incTime=2*60, EBtim
    #super(StoppableThread, self).__init__()
    bt.BasicThread.__init__(self, Period=Period, nameID=nameID)
    self.setup = setup
    self.reset()
    self.incTime = incTime
    self.EBtime = EBtime
    self.EB2time = EB2time
    self.Elutions = Elutions
    def reset(self):
        self.pause()
        self.state = 'Washing1'
        self.subState = ''

    def process(self):
        ## \ Code begins below \
        print '%s: %s / %s'%(self.name, self.state, self.subState)
        ###STATE1###
        if self.state == 'Washing1':
            if self.subState == '':

```

Ln: 1 Col: 0

- g. Add protocols to move the droplets by studying the electrode numbers of the chip and save it(optional).

```

protocol_Alen.py - G:\Alen\Design1\Codes\protocol_Alen.py (2.7.14)
File Edit Format Run Options Window Help
seqList = [[34, 31, 7], [31, 7, 30], [7, 30, 6], [6, 30, 29],[29]] # <--
seqOnTime=0.7 # <-- How long is the electrode actuated [Sec]
seqPeriod=1 # <-- Keep this at least 0.2 seconds above onTime [Sec]

self.seqAdd(seqCategory, seqName, seqDesc, seqList, seqPeriod, seqOnTime
# /\ ** END OF SEQUENCE ** /\

# \/ ** START OF SEQUENCE ** \/
seqCategory = 'Solid Phase Extraction' #<-- EDIT THIS
seqName = 'Apt1 to det1' #<-- EDIT THIS
seqDesc = '' #<-- EDIT THIS
seqList = [[29, 87,88], [87, 88, 65], [65]] # <-- Electrodes 1 and 2 act
seqOnTime=0.7 # <-- How long is the electrode actuated [Sec]
seqPeriod=1 # <-- Keep this at least 0.2 seconds above onTime [Sec]

self.seqAdd(seqCategory, seqName, seqDesc, seqList, seqPeriod, seqOnTime
# /\ ** END OF SEQUENCE ** /\

# \/ ** START OF SEQUENCE ** \/
seqCategory = 'Solid Phase Extraction' #<-- EDIT THIS
seqName = 'Apt1 to det2' #<-- EDIT THIS
seqDesc = '' #<-- EDIT THIS
seqList = [[29, 87,88], [87, 88, 65], [88, 65, 90], [65, 90, 66], [90, 6
seqOnTime=0.7 # <-- How long is the electrode actuated [Sec]
seqPeriod=1 # <-- Keep this at least 0.2 seconds above onTime [Sec]

self.seqAdd(seqCategory, seqName, seqDesc, seqList, seqPeriod, seqOnTime
# /\ ** END OF SEQUENCE ** /\

# \/ ** START OF SEQUENCE ** \/
seqCategory = 'Solid Phase Extraction' #<-- EDIT THIS
seqName = 'Apt2 to det4' #<-- EDIT THIS
seqDesc = '' #<-- EDIT THIS
seqList = [[34,67, 91], [67, 91, 68], [91, 68, 92], [68, 92, 69], [92, 6
seqOnTime=0.7 # <-- How long is the electrode actuated [Sec]
seqPeriod=1 # <-- Keep this at least 0.2 seconds above onTime [Sec]
Ln: 11 Col: 0

```

Note: The below images show the electrode numbers of the chips. All the necessary codes to move the droplets are incorporated in the protocol.py. However, if additional movements are to be achieved, add them in the protocol file.

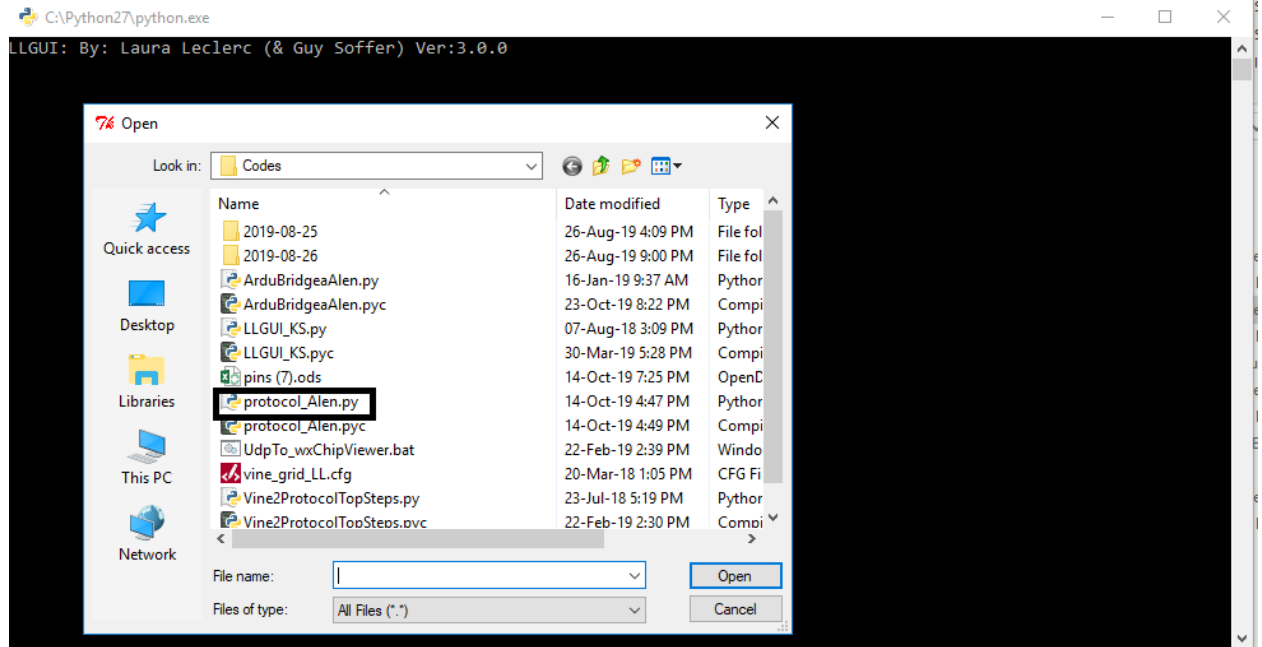
			48					5					33					15			
			49					28					10					38			
			50					27					9					14			
			51				26	3				8	32			13	37				
53	54	55	52	86	25	2	63	29	6	30	7	31	34	11	35	12	36	39	16	40	17
			85					87					67					70			
			84					88					91					94			
			83					65					68					71	98	75	99
			59					90					92					95			
56	57	58	82					66					69					72			
								89					93					96	73	97	74

Figure 1: Chip Design 1 with Pin Out

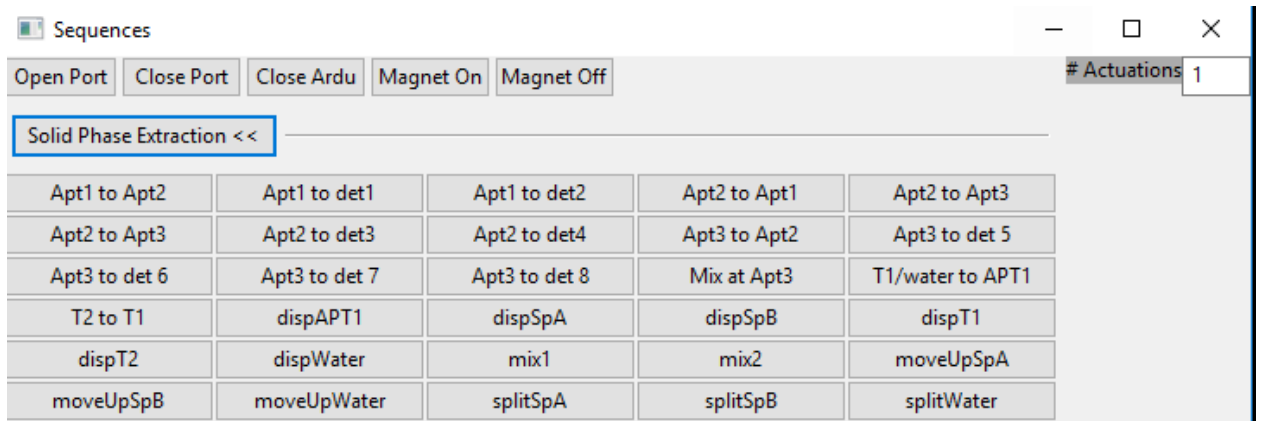
			48									10						20						
			49									33						43						
			50				28					9			38			19	44	21	45			
			51				4					32			14			42						
			52	1	2	3	5	29	30	31	34	11	12	13	15	39	40	41	99					
57	56	55	54	53	60	25	26	27	87	6	7	8	67	35	36	37	70	16	17	18	97	74	98	75
			58	83	84	61	85	63	64	88	65	90	91	68	92	94	71	95	72					
			82				62					89			69			73						
			59				86					66			93			96						

Figure 2: Chip Design 2 with Pin Outs.

- h. Open and run the file LLGUI.py and upload the protocol.py file. This creates a GUI for copying the functions to initiate the droplet motion.



- i. Click on the required droplet motion.



- j. The copied function can be pasted on the terminal in step “i”.

```
type prot.start() to run protocol. Start LLGUI or ChipViewer to control droplet
movement.
>>> setup.seq['dispSpA'].start(1)|
```

- k. Press **ENTER** on the terminal. This will initiate the required droplet motion.

5. Running the experiments on the chip:

- a. After setting up the hardware as in step “4”, pipette the ribozyme solutions (2 μ L) on the reservoirs.

- b. Pipette 2 μL of cleavage buffer on the detection points.
- c. Carefully place and stick the top plate to the DMF chip and make sure that the top plate is connected to H_GND.
- d. Setup the software as detailed in step “5”.
- e. Initiate the step to dispense the Ribozyme droplet.
- f. Move the droplet to the desired detection point with the cleavage buffer.
- g. Mix the droplet at the detection point by moving the assayed droplet up and down.

Note: All the functionality to achieve droplet motion can be copied using the GUI.

Reading fluorescence

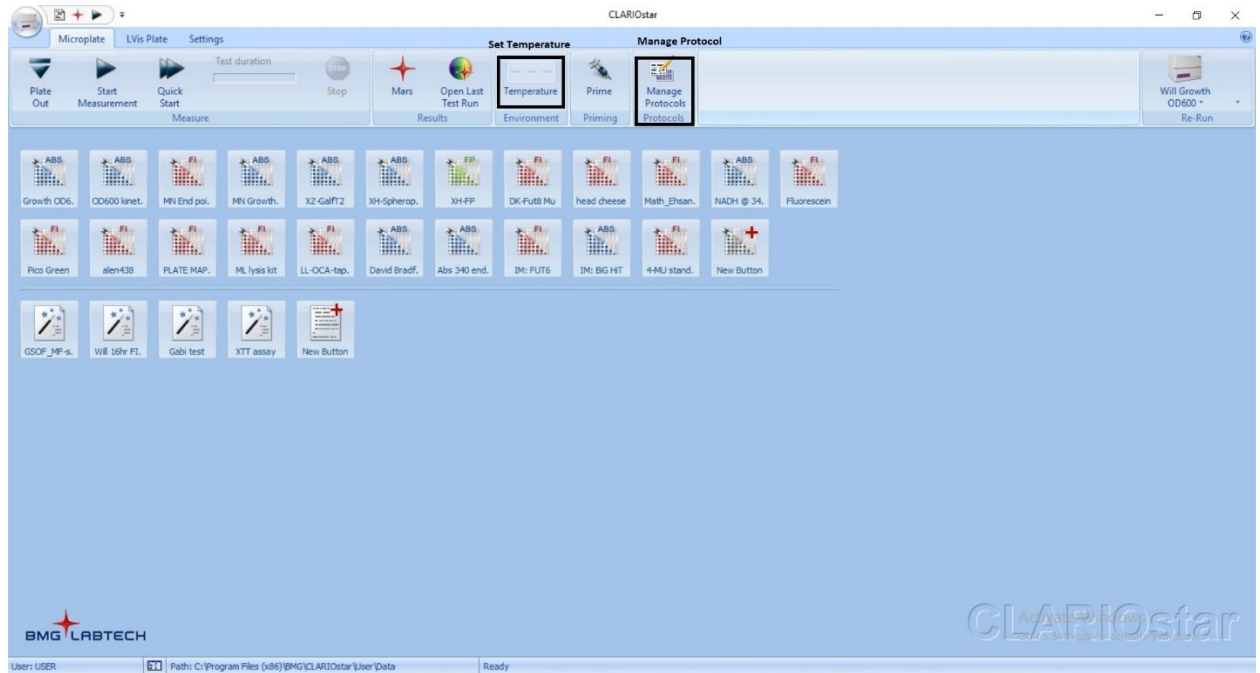
Required Materials

Item	Stock Quantity/Concentration
Plate reader	
Well plate (with or without DMF chip)	

Procedure

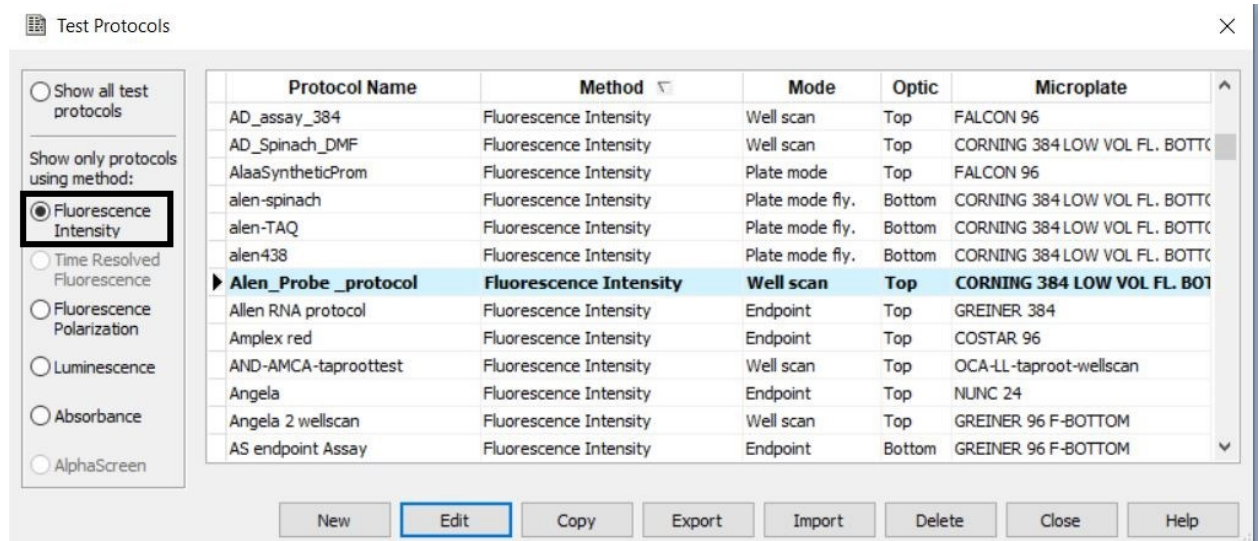
1. Reading fluorescence
 - a. Place the well-plate in the ClarioStar plate reader.
 - b. Set the temperature to 37°C.

c. From the UI (User interface) click on **Manage Protocols**.



d. On the left tab of the new window, select **Fluorescence Intensity**.

e. Select on **Alen_Probe_protocol** and click on **Edit**.



f. Select the type of microplate (or well-plate).

g. Set the fluorophore to be **Cy5**.

h. Make sure that the excitation and emission wavelengths are set to **610-30** and **675-50**, respectively.

i. Set the optics to **Top optic**.

j. Click on **Start measurement**.

Fluorescence Intensity - Well Scan

Basic Parameters | Layout | Concentrations / Volumes / Shaking

Step f.

Protocol name:

Microplate:

Focal height (0...25.0 mm):

Step g.

Optic Settings

No. of multichromatics (1...5): +

Presets:

Step h.

Excitation: Dichroic: Emission:

General Settings

Setting time (0.0...1.0 s):

Measurement start time (0...1200 s):

No. of flashes per scan point (0...200):

Well Scan

Scan matrix: Diameter (1...2 mm):

Step i.

Optic

Top optic Bottom optic

Step j.

k. Select the wells to be scanned and can be changed by clicking the **change layout button**.

l. Check the **focus** and **gain** adjustments and click on **Start Adjustments**, to automatically set the focal length.

Start Measurement - Alen_Probe_protocol

Focus and Gain Adjustment / Plate IDs Sample IDs / Dilution Factors

Change layout Use this to select the wells to be scanned

384	1	2	3	4	5	6	7	8	9	10	11	12	13	14	15	16	17	18	19	20	21	22	23	24
A																								
B																								
C																								
D																								
E																								
F																								
G											X1	X2	X3	X4	X5									
H											X6	X7	X8	X9	X10									
I											X11	X12	X13	X14	X15									
J											X16	X17	X18	X19	X20									
K											X21	X22												
L																								
M																								
N																								
O																								
P																								

Focus and Gain Adjustment

Monochromator / Filter Settings		Gain
1	610-30/675-50	1800

Focus Adjustment

Eocal height (0...25.0 mm): 15.0

Gain Adjustment

Selected well Target value: 90 %

Full plate

0 50 100% 200,000

Check both Focus adjustment and Gain Adjustment to automatically set up the gain and focus

Raw result: Step I.

Start Adjustment Stop Adjustment

Status: Ready

Plate Identification

ID1: ID2: ID3:

Automatically enter the plate IDs previously used with this protocol

No. of executed runs since program start: 94 Total no. of executed runs: 7786

Clear IDs Get last IDs

Run statistics: Go to Settings

Start measurement Save & Close Cancel Help

m. After adjusting the scan, click on **Start measurement** to initiate the well-scan.

CLARIOstar

Microplate LVis Plate Settings Step n.

Plate Out Start Measurement Quick Start Test duration Stop Mars **Open Last Test Run** Temperature Prime Manage Protocols Will Growth OD600 Re-Run

Growth OD6. ABS. CD600 line1. MN End pos. MN Growth. X2-GalT2. X1-Spherop. X1-PP. DK-Fu18 Mu. head cheese. Math_Ehsan. NADH @ 34. Fluorescen.

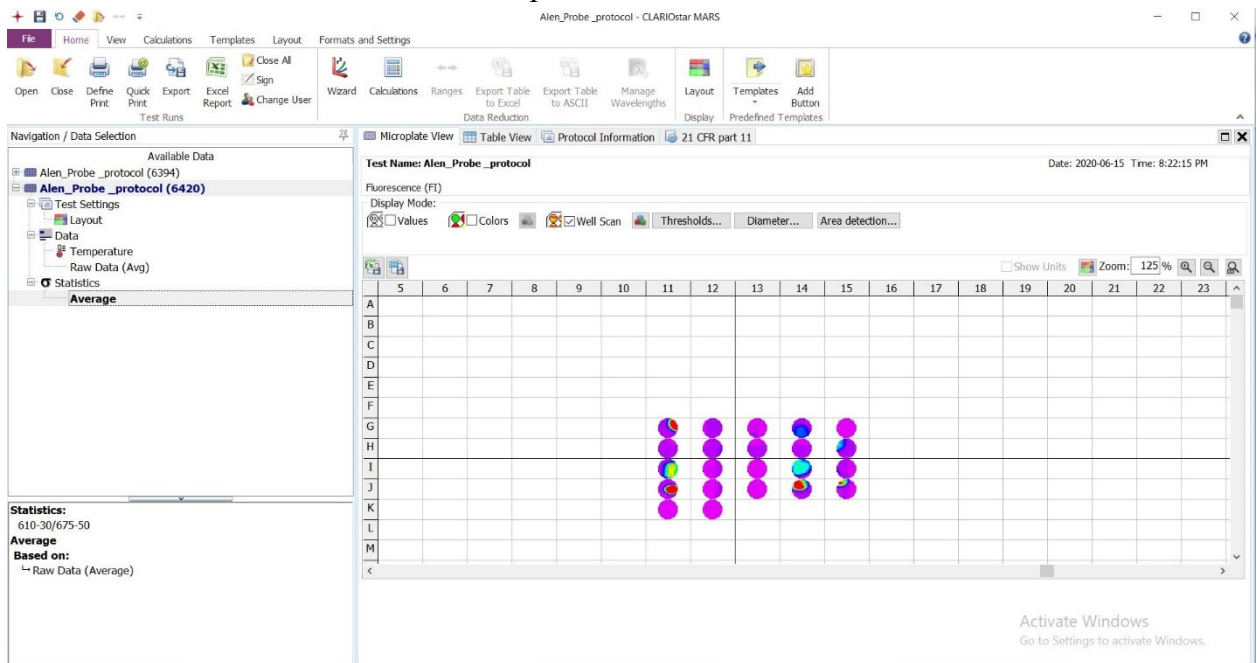
Pico Green. allen-438. PLATE MAP. Ml. lysis kit. LL-OCA-top. David Bradf. Abs 340 end. IM: FLTG. IM: BIG HT. 4-MJ stand. New Button

GSDP_MF-s. WII 16V FL. Gabi test. XTT assay. New Button

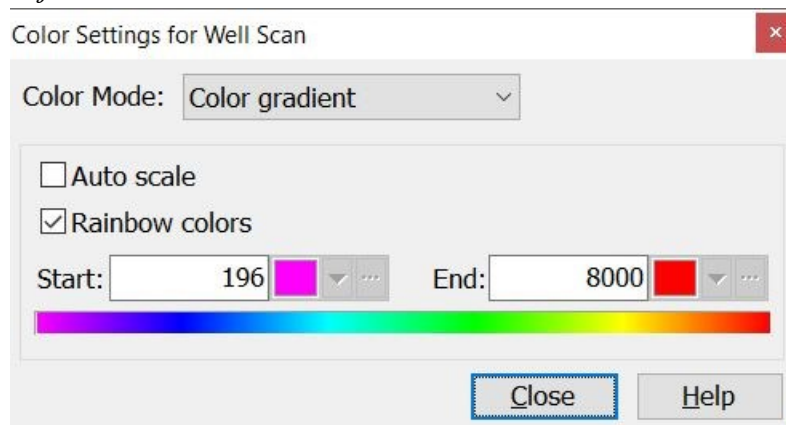
BMG LABTECH CLARIOstar

User: USER Path: C:\Program Files (x86)\BMG\CLARIOstar\User\Data Ready

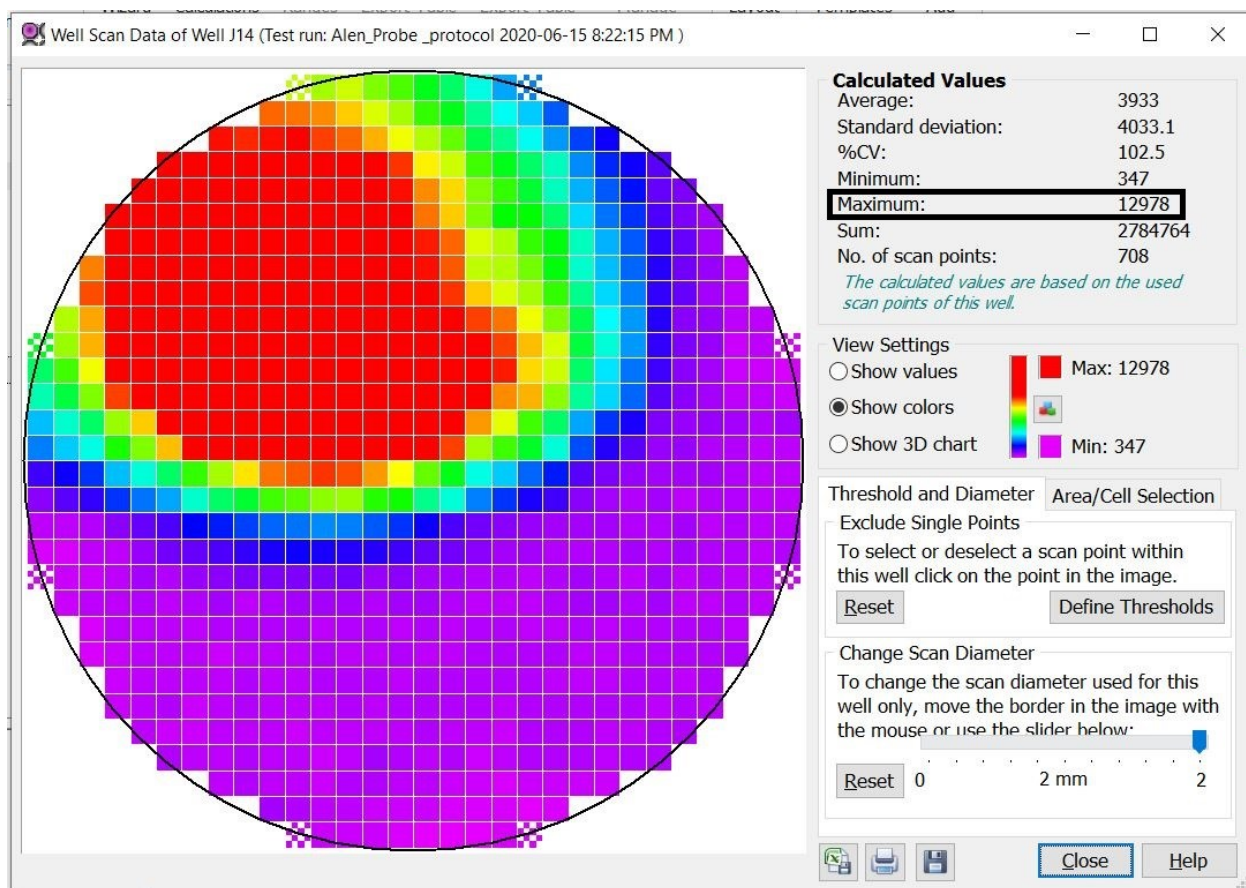
- n. After scanning the wells, open the data in **MARs** by clicking **Open Last Test Run**.
- o. The data will be indicated as heat map of the well-scans.



Note: If the droplets are not visible. Please change click on the button next to Threshold bar. This opens a window, change the layout to rainbow colors and adjust the Start and End values.



- p. Double click the wells, which opens a new window with the fluorescence values at different positions within the well.



- q. Note the **Maximum fluorescence** intensity of each well.
- r. Record the Maximum fluorescence intensity of each well and the time it took to scan the wells in an excel sheet.
- s. Repeat steps “c-r” to get the required number of readings.
Note: Reading the fluorescence can also be initiated by clicking the re-run protocol option on the ClarioStar UI. Thereafter, the readings can be visualized by following steps “n-r”.

